polymers

MDPI

Review

A Review on Hydrogels with Photothermal Effect in Wound Healing and Bone Tissue Engineering

Xu Zhang, Bowen Tan, Yanting Wu, Min Zhang and Jinfeng Liao *

State Key Laboratory of Oral Diseases, National Clinical Research Centre for Oral Diseases, West China Hospital of Stomatology, Sichuan University, Chengdu 610041, China; zx2020224030006@163.com (X.Z.); bowentan711@163.com (B.T.); yantingwu0521@outlook.com (Y.W.); zhangmin5477@163.com (M.Z.)
* Correspondence: liaojinfeng.762@scu.edu.cn

Abstract: Photothermal treatment (PTT) is a promising strategy to deal with multidrug-resistant bacteria infection and promote tissue regeneration. Previous studies demonstrated that hyperthermia can effectively inhibit the growth of bacteria, whereas mild heat can promote cell proliferation, further accelerating wound healing and bone regeneration. Especially, hydrogels with photothermal properties could achieve remotely controlled drug release. In this review, we introduce a photothermal agent hybrid in hydrogels for a photothermal effect. We also summarize the potential mechanisms of photothermal hydrogels regarding antibacterial action, angiogenesis, and osteogenesis. Furthermore, recent developments in photothermal hydrogels in wound healing and bone regeneration applications are introduced. Finally, future application of photothermal hydrogels is discussed. Hydrogels with photothermal effects provide a new direction for wound healing and bone regeneration, and this review will give a reference for the tissue engineering.

Keywords: hydrogel; photothermal effect; antibacterial; angiogenesis; wound healing; bone regeneration

Citation: Zhang, X.; Tan, B.; Wu, Y.; Zhang, M.; Liao, J. A Review on Hydrogels with Photothermal Effect in Wound Healing and Bone Tissue Engineering. *Polymers* **2021**, *13*, 2100. https://doi.org/10.3390/polym13132100

Academic Editors: Dimitrios Bikiaris, Ashveen Nand and Sudip Ray

Received: 24 May 2021
Accepted: 19 June 2021
Published: 25 June 2021

Publisher's Note: MDPI stays neutral with regard to jurisdictional claims in published maps and institutional affiliations.

Copyright: © 2021 by the authors. Licensee MDPI, Basel, Switzerland. This article is an open access article distributed under the terms and conditions of the Creative Commons Attribution (CC BY) license (http://creativecommons.org/licenses/by/4.0/).

1. Introduction

Tumors [1], fractures [2], burns [3], diabetes [4], and other acute/chronic diseases seriously affect people's health. These diseases are accompanied by severe infections or tissue defects. In clinical practice, doctors use large doses of antibiotics to control infection and artificial substitutes to repair tissue defects. However, this may lead to the emergence of drug-resistant bacteria and tissue inflammation around implants. With the rapid development of bio-nanotechnology, researchers have developed various kinds of biomaterials such as hydrogels [5], films [6], sponges [7], cements [8], microneedles [9], and three-dimensional (3D)-printed scaffolds [10] to solve these problems.

Hydrogels, as a 3D porous material, can keep a moist microenvironment, absorb inflammation exudate, and provide a physical barrier to prevent bacteria from entering the wound [11,12]. Other features of hydrogels include their excellent biocompatibility, adjustable degradation properties, and proper mechanical properties [13,14]. Researchers have developed different kinds of hydrogels that are suitable for different defect sites. Injectable hydrogels can complete sol-gel conversion in a short time via hydrogen bonds [15,16], host–guest interactions [17], dynamic Schiff bonds [18], dynamic diol-borate ester crosslinking [19], and the Diels–Alder reaction [20]. Hence, injectable hydrogels can be applied to irregular defect areas. However, external shear stress may destroy the internal structure of hydrogels, and even lead to gel-sol conversion. Hydrogels polymerized from monomers have excellent stability and high mechanical strength. The cross-linked hydrogels are synthesized mainly by polymerization with carbon–carbon double bonds. The

monomers used commonly are acrylamide [21], N-isopropylacrylamide [22,23], and gelatin methacrylate (GelMA) [24]. Moreover, ionic cross-linking hydrogels, such as Ca^{2+} cross-linked sodium alginate hydrogel, has attracted much attention because of its convenient cross-linking and stable performance [25,26]. Hydrogels mimic the extracellular matrix to promote cell proliferation and further accelerate tissue regeneration [27].

Several recent studies have focused their attention on changes in the external temperature that influence the responses of bacterial, cells, and tissues. Photothermal agents can convert light energy to heat under near infrared (NIR) irradiation [28,29]. The target temperature of photothermal hydrogels can be adjusted by changing the concentration and proportion of photothermal agents, irradiation time, and laser intensity [30]. Mild local heat (41 °C–43 °C) can promote cell proliferation, angiogenesis, wound healing, and bone regeneration [31]. Moderate heat (45 °C–50 °C) causes negligible damage to normal tissue cells in a short time but fatal damage to tumor cells [32–34]. For infected wound healing, hyperthermia (>50 °C) can effectively inhibit the proliferation of bacteria. Therefore, photothermal effects can be controlled for different applications based on different temperature.

The change in temperature can control the gel-sol transformation of thermosensitive hydrogels and release active factors for enhanced therapy [35]. Pedersen et al. reported that a polyvinyl alcohol/gold nanorod (AuNR) hydrogel was heated to <50 °C under NIR irradiation and liquefied in 15–20 s, and the pulsed release model cargo of fluorescein isothiocyanate controlled by NIR irradiation was realized successfully [36]. Under NIR irradiation, [poly(D,L-lactide)-poly(ethylene glycol)-poly(D,L-lactide)/black phosphorus (BP) hydrogel undergo a sol-gel transition at 46.5 °C after only 20 s [37]. Hyperthermia (>50 °C) could destroy the integrity of bacterial cell membranes, cause protein denaturation, and finally kill bacteria [38]. Hyperthermia caused by long-term exposure to NIR laser can also result in irreversible damage to normal tissues. To minimize the negative influence on normal tissues, antibacterial substances are usually incorporated into hydrogels to work with photothermal effects. Hydrogels can load drugs via hydrogen bonds [39], π−π stacking [40], dynamic chemical bonds [41], and electrostatic absorption [42,43]. Furthermore, hyperthermia can effectively alleviate intermolecular forces or shrink volume to achieve rapid drug release to enhance the therapeutic effect [44–47].

Therefore, photothermal hydrogels combine the advantages of traditional hydrogels with the effect of temperature stimulation on tissues. Controlling the final temperature of the hydrogels enables them to be used in different biological treatment strategies. Different types of hydrogels can be selected according to the application sites and therapeutic strategies. In this review, the fabrication and characteristics of photothermal hydrogels are introduced. Photothermal hydrogels showed good applications in wound healing and bone regeneration in recent years. Furthermore, the future perspective of photothermal hydrogels in the biomedical field is discussed.

2. Composition of Hydrogels with Photothermal Effects

Materials with photothermal effects have been applied widely in antitumor treatment, and increasing applications in antibacterial effect, wound healing, and tissue regeneration have been reported in the past 2–3 years [48]. According to the different sources of photothermal initiators, materials with photothermal effects can be divided into two types: inorganic materials and organic materials. Inorganic materials are usually nanomaterials and show strong NIR absorption properties and possess a stable photothermal effect. However, a high concentration of nanomaterials may be toxic to tissue and easy to aggregate. Compared with inorganic materials, organic materials show approving biocompatibility and are readily available. However, organic materials with photothermal effect often have photobleaching effect. In the following sections, hydrogels with different kinds of photothermal agents are introduced systematically.

2.1. Inorganic Materials Hybrid Hydrogels with Photothermal Effects

The inorganic materials with photothermal effects include carbon nanotubes [49–51], reduced graphene oxide (rGO) [52,53], gold nanoparticles [54–56], BP [57,58], AuPds [31], silver [59], TiO_2 [60], and platinum nanoparticles [61]. However, the aggregation of nanoparticles in organisms limits their applications. Hydrogels with a porous network have been used widely in biomedicine. One of the strategies to solve aggregation is that nanomaterials can be dispersed effectively in hydrogels [62,63]. In addition, nanomaterials can be surface-modified and covalently cross-linked or non-covalently cross-linked with hydrogels [64,65].

Chitosan (CS)/antimonene nanosheets (AMNSs) hydrogels were prepared via a bidirectional freeze-casting approach by Liu's group. Scanning electron microscope (SEM) images showed that the layered AMNSs were embedded evenly in the framework of the CS hydrogel [66]. GO lacks stability in a physiological cycle. Surface modification could improve its stability and further form a covalent bond with the bulk of the hydrogel. The amino group can be obtained by grafting branched poly-ethylenimine (BPEI) onto graphene oxide, which could be cross-linked with the aldehyde group to form a dynamic Schiff base bond [67]. Some metal–organic frameworks have been developed for photothermal therapy. For example, N, N-bis (acryloyl) cystamine can effectively adsorb copper nanoparticles via Cu–S bonds [68]. Moreover, polyvinyl pyrrolidone (PVP) functionalized GO nanosheets were crosslinked with AuNRs via non-covalent electrochemical interactions. Then PVP-nGO@AuNRs can be added into interpenetrating network (IPN) formed hybrid hydrogel by free radical polymerization [55]. To avoid nanomaterials aggregation, Prussian blue (PB) can be surface modified by PDA to anchor Ag^+ and achieve controlled release Ag^+. Moreover, due to high photothermal conversion property and excellent stability of PB, PB has been applied in antibacterial therapy and wound healing [69,70].

2.2. Organic Materials Hybrid Hydrogels with Photothermal Effects

Organic materials with photothermal conversion ability have also received extensive attention because of their good degradation properties and excellent biocompatibility. Research studies on organic photothermal conversion materials focused on dyes such as IR-820 [71,72], IR-780 [73,74], indocyanine green (ICG) [75], and conjugated polymers such as poly-dopamine (PDA) [76,77], poly-pyrrole [78,79], and poly-aniline [80].

Dopamine (DA), as a material with excellent photothermal conversion and adhesion abilities, has attracted increasing attention. DA can be grafted onto polymer materials, such as GelMA [81], hyaluronic acid(HA) [82], and bioactive glass nanoparticles (BGNs) [83], to improve its adhesion ability. In addition, DA could chelate with other photothermal materials (such as Cu^{2+} [84], and Ti [85]) to increase the photothermal performance of hydrogels. Furthermore, the catechol group can be easily oxidized to the catechol–quinone group, which further forms chemical cross-links to improve the mechanical properties of hydrogels [86,87]. PDA can be finally formed by oxidative and DA self-polymerization in a basic solution [88]. PDA can load the drug through $\pi-\pi$ stacking, hydrogen bonds, and electrostatic attraction. Tong et al. recently fabricated Curdlan powder/PDA hydrogel and successfully loaded chlorhexidine (CHX). CHX is an antibacterial drug, and was used to gain a controllable NIR-triggered release [89]. Moreover, PDA can be incorporated with GO through $\pi-\pi$ stacking to regulate the NIR-triggered release and reduce drug leakage [90].

ICG [41,91], as an FDA-approved photothermal therapeutic agent, has also attracted increasing attention owing to its remarkable photothermal conversion efficiency. ICG can also improve photothermal therapeutic effects by incorporating rare-earth nanoparticles (Ln: 72% Y^{3+}, 20% Yb^{3+},8% Tm^{3+}) via electrostatic adsorption. Li et al. recently created an ICG–rare-earth nanoparticle-loaded hydrogel, with the successful implementation of NIR-triggered release of adriamycin (DOX) [92].

3. Potential Mechanisms of Photothermal Hydrogels for Wound Healing and Tissue Engineering

To achieve the flexible use of photothermal hydrogels in wound healing and bone tissue engineering, it is necessary to explore the potential mechanisms of photothermal effects in antibacterial activity, angiogenesis, and osteogenesis. Mild local heat can improve the expression of various genes that promote tissue repair, thereby promoting cell proliferation and differentiation, and ultimately accelerating wound healing and bone regeneration. In wound healing and bone regeneration, oxygen and nutrition supply from neovascularization is essential. When the wound is seriously infected, antibodies in the blood can control the infection. Based on controlling infection and angiogenesis, bone marrow mesenchymal stem cells (BMSCs) can proliferate and further promote tissue regeneration.

3.1. Antibacterial Effects

Recent researches disclosed that high temperature (>50 °C) can effectively kill bacteria [93]. Hence, materials with high photothermal conversion efficiency have gradually caught the attention of researchers. High temperature could cause enzyme inactivation, cell membrane permeability changes [66,82], cytoplasmic outflow [66], and protein denaturation [94] (Figure 1). The cell membranes of *Escherichia coli* became shrunken and blurred after NIR irradiation, and the integrity of the cell membranes was destroyed, indicating that high temperature can destroy bacterial cell membranes [95]. Moreover, Li et al. demonstrated that the photothermal effect can destroy bacterial cell membranes, denature bacterial proteins, and change cell membrane permeability [96]. Further, the bacterial intracellular matrix flowed out when the integrity of the cell membranes and cell walls was destroyed. Using transmission electron microscopy, Liu et al. found that the bacterial cell membranes were destroyed, resulting in cytoplasm outflow [97].

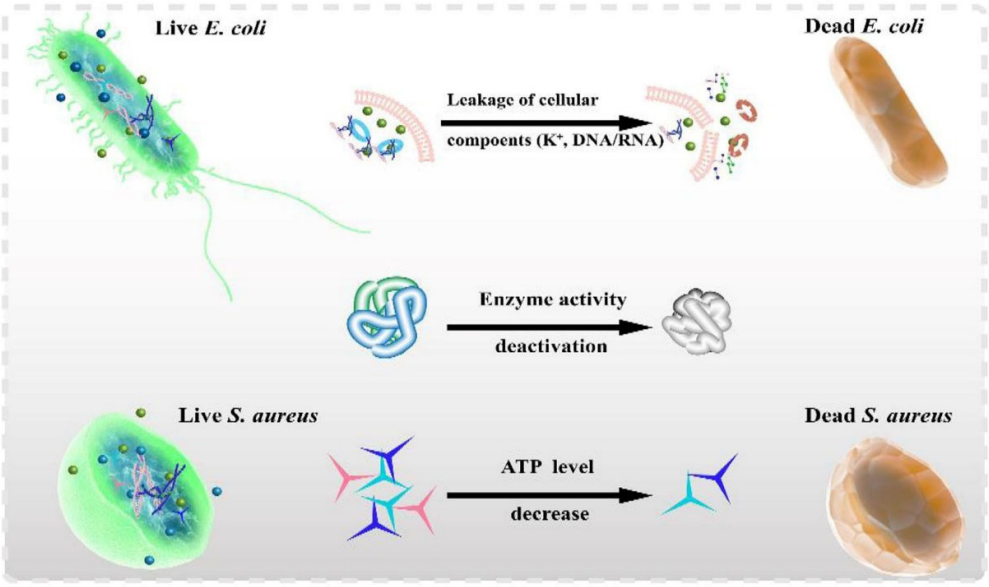

Figure 1. Hyperthermia effects on the antibacteria via changing cell membrane permeability, enzyme inactivation, and protein denaturation [95]. Copyright 2021, Elsevier.

In the application of photothermal therapy, hyperthermia recovers to body temperature in a short time. To improve the treatment efficacy, strategies include increasing the irradiation time and adding bioactive agents for co-therapy. Photothermal antibacterial materials can be combined with various antibacterial substances, (such as Cu_2O [98], Ag^+ [99,100], and Au [101]), to increase antibacterial effect. The antimicrobial metal ions and

metal oxides can act synergistically with photothermal materials to increase the antimicrobial properties of the composite material. A "one stone, two birds" strategy was used, based on the surface plasmon resonance (SPR) effect of Ag^{+} and Cu^{2+} to kill bacteria by photothermal therapy and achieve a sustained and stable release of bioactive ions with antibacterial properties [102,103]. Interestingly, in another study, copper ions were incorporated with NIR irradiation, and bacteria were inhibited quickly and continuously because of the "hot ions effect". Cyclic NIR irradiation was used to verify the antibacterial properties of the hot ions effect. In the first cycle, the antibacterial activity of a PDA/Cu hydrogel against *E. coli* reached 88.37%, whereas the Cu group showed poor antibacterial activity (9.30%). After the second NIR irradiation cycle of 2 h, the antibacterial rate of the PDA/Cu hydrogel was 98.53%, whereas the antibacterial rate of the hydrogel without NIR irradiation was 79.48% [84]. Moreover, the CuS/MoS_2/PVA hydrogel could produce hyperthermia and reactive oxygen species under NIR/visual light to provide an antibacterial treatment. As shown in Figure 2, after the bacteria were incubated with the hydrogel, the cell membranes were damaged to varying degrees [104]

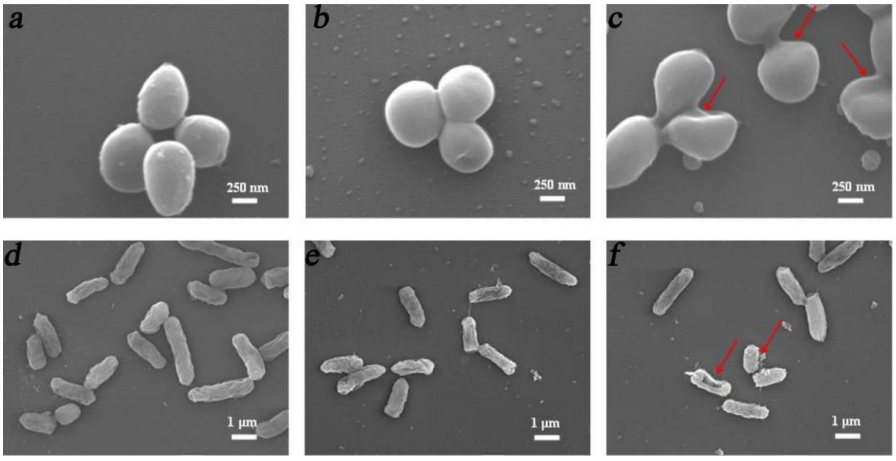

Figure 2. SEM images of S. aureus (**a**–**c**) and *E. coli* (**d**–**f**) after culture on PVA/CuS/MoS_2 hydrogels with NIR/visual light irradiation for 15 min. (**a**,**d**) PVA hydrogel, (**b**,**e**) CuS incorporated PVA hydrogel, and (**c**,**f**) CuS/MoS_2-incorporated PVA hydrogel [104]. Copyright 2020, Elsevier.

Hydrogels can be incorporated with drugs to improve antibacterial properties via π−π stacking, reversible covalent cross-links [105], and direct encapsulation [106]. A photothermal trigger or pH trigger can be chosen to control drug release [107]. Liu et al. revealed that MPDA/GO/CNF composite hydrogel could be easily loaded with tetracycline hydrochloride (TH) via π−π stacking and hydrogen bonds. When the pH changes from a neutral to an acidic condition, the amino group on the surface of PDA changed from deprotonation to protonation, further disrupting the attachment between TH and PDA. In addition, hyper-temperature could alleviate π−π stacking to achieve a rapid release of TH [90]. Curcumin is an aromatic hydrocarbon material used widely for its anti-inflammatory, antibacterial, and antitumor activities [108]. A gel-PDA/Cur hydrogel could form π−π stacking with curcumin. Under NIR irradiation, curcumin can be released rapidly compared to only a slight release without NIR. This phenomenon can be attributed to the fact that π−π stacking and hydrogen bonds can be destroyed by hyperthermia [95,109]. Doxycycline, as a broad-spectrum antibiotic agent, has been used widely in clinical practice [110]. The amino group on doxycycline can form a hydrogen bond with HA-DA/rGO hydrogel to prolong the drug release time [93]. Yang et al. constructed dodecyl-modified CS/PEG–CHO/Tungsten disulfide nanosheets hydrogel to load ciprofloxacin *via* hydrogen bonding and electrostatic interactions, and NIR-triggered ciprofloxacin release was achieved successfully [111].

3.2. *Angiogenesis*

In chronic wound healing and bone tissue repair, hypoxic cells are usually unable to proliferate normally owing to lack of nutrients. Angiogenesis can provide oxygen and nutrients to the newborn tissue, thus helping to accelerate wound healing and bone repair. Recent studies have found that mild heat (40 °C–41 °C) can effectively increase the vascular density in the new granulation tissue by inducing the proliferation of vascular endothelial cells. Moreover, by simulating the "hot spring effect", mild heat can be incorporated with Fe^{2+}, SiO_4^{4-} ions to regulate the expression of vascular genes such as hypoxia inducible factor-1 (HIF-1α), vascular endothelial growth factor (VEGF), endothelial nitric oxide synthase (eNOs), basic fibroblast growth factor (bFGF), and further promote circulation of blood (Figure 3) [112]. Moreover, Cu^{2+} and Mo^{4+} ions could promote angiogenesis by promoting the expression of related genes (VEGF, KDR, HIF-α, eNOs, bFGF) [68,84]. HIF-α can mimic hypoxia environment to induce cell differentiation. Some ions, such as Cu^{2+}, Mo^{4+}, and SiO_4^{4-}, can also promote collagen deposition, hair follicle regeneration, and fibroblast proliferation, and accelerate tissue healing [113–115].

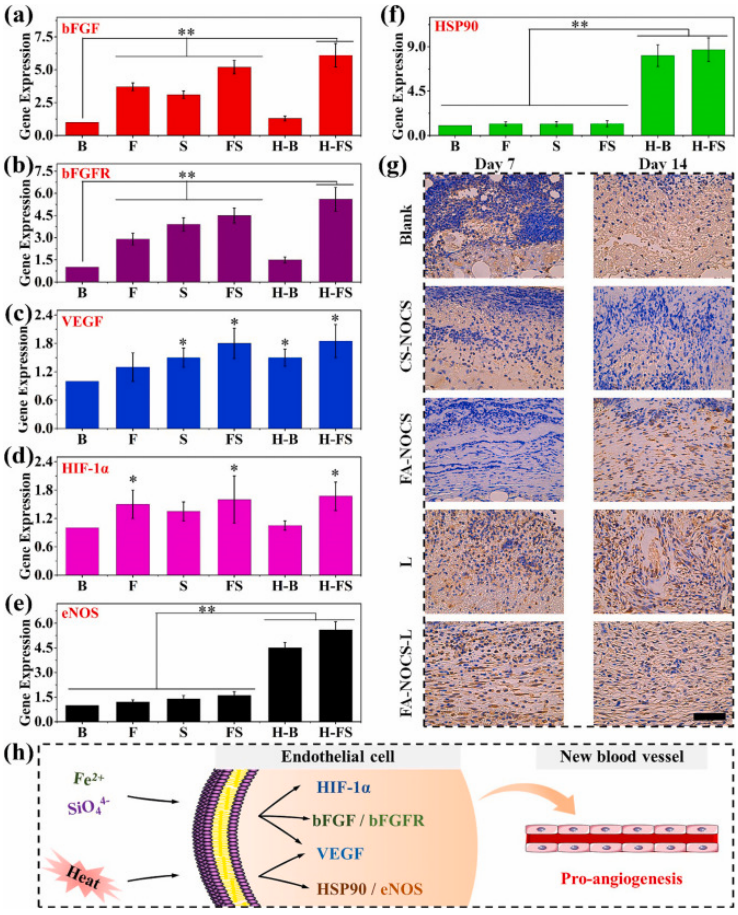

Figure 3. The effect of heat stimulation and Fe/Si ions on gene (in vitro) and protein (in vivo) expression. (**a**) bFGF, (**b**) bFGFR, (**c**) VEGF, (**d**) HIF-1α, (**e**) eNOS, (**f**) HSP90 gene expression of HUVECs at day 7. (**G**) Immunohistochemical staining for HSP90 (Blank: no treatment; CS-NOCS: calcium silicate-NOCS composite hydrogels without NIR irradiation; FA-NOCS: FA-NOCS composite hydrogels without NIR irradiation; FA–NOCS–L: FA-NOCS composite hydrogels with NIR irradiation (808 nm, 0.36 W/cm^2, 15min/day, day 1–5); L: laser irradiation only; Bar = 50 μm). (**h**) Possible activation mechanism of the combined effect of ions and thermal stimulation on angiogenesis. (B: blank; F: Fe^{2+} containing medium; S: SiO_4^{4-} containing medium; FS: Fe^{2+} and SiO_4^{4-} containing medium; H–B: heat treatment; H-FS: combination of heat and Fe^{2+} and SiO_4^{4-} ion treatment, * $p < 0.05$, ** $p < 0.01$). [112] Copyright 2020, Elsevier.

Adequate oxygen could promote cell proliferation and tissue regeneration. However, it is difficult for most oxygen carriers to release oxygen into deep tissues [116]. In addition, CO_2 can stimulate angiogenesis in the wound area via the Bohr effect. The Bohr effect means that the hemoglobin releases more oxygen when the pH of the blood decreases. Bicarbonate decomposes into CO_2 under mild heat (42 °C). Bicarbonate can be coordinated with Fe^{3+} and bound to the PDA hydrogel network, further achieving the controlled release of CO_2 triggered by photothermal conversion [117,118]. Moreover, NO, an important signal regulation molecule, could promote angiogenesis via multiple mechanisms [119]. Recent research suggested that excess NO did not show satisfactory results compared to a small quantity of NO, and excessive NO release of NO may inhibit cell proliferation. So, controlled NO release is a key factor in its application. As a material that can continuously release NO under NIR irradiation, the hydrophobic BNN6 limits its application. Hydrogels as a hydrophilic 3D network structure material carrier can encapsulate hydrophobic agents to disperse them well [82,120]. Zeolitic imidazolate framework-8 (ZIF-8), as a novel metal–organic framework, could absorb many small molecules because of its positively charged surfaces and efficiently improve water solubility. Liu et al. recently successfully achieved the NIR-controlled release of NO by encapsulating ZIF-8@BNN6 nanoparticles in a GelMA/oxide dextran hydrogel. With the increase in the number of NIR irradiation cycles, the NO produced by the decomposition of BNN6 exhibited a cumulative effect [121].

3.3. Osteogenesis

Compared with short photothermal stimulation without obvious effects on osteogenesis, periodic photothermal treatment can stimulate the proliferation and differentiation of BMSCs, which are attributed to the prolongation thermal effect. Mild heat stimulation (41 °C once a week for 1 h) could enhance the expression of alkaline phosphatase (ALP) to promote BMSCs differentiation into osteoblasts [122]. Some direct proofs also showed that weekly photothermal stimulation after 10 weeks can promote bone regeneration efficiently in vivo. Micro-computed tomography images showed that the bone volume/total volume (BV/TV) ratio of the NIR irradiation + poly (lactic-co-glycolic acid) (PLGA) group was 23.50% ± 1.12% and that of the only PLGA group was 12.02% ± 1.30% [57]. Moreover, under NIR irradiation stimulation, osteocalcin, a late osteogenic differentiation marker, can be overexpressed by activating the Wnt signaling pathway. Mild heat stimulation activates the Wnt signaling pathway by up-regulating the expression of Wnt10b and A1p1 genes to stimulate bone regeneration [31].

BP, as an excellent photothermal conversion agent, can be oxidized to PO_4^{3-} and form calcium phosphate (CAP) with calcium for in situ mineralization (Figure 4) [123,124]. CAP has excellent mechanical properties, which can be applied in bone defects of weight-bearing area [125]. Moreover, PO_4^{3-} could promote osseointegration by being incorporated with Gd^{3+}. The mechanism is as follows: (1) stimulate the M2 polarization of macrophages by releasing Gd^{3+}; (2) promote angiogenesis by up-regulating VEGF in M2 polarized macrophages; and (3) achieve the deposition of calcification analogous to the Haversian system around the neovascularization [126].

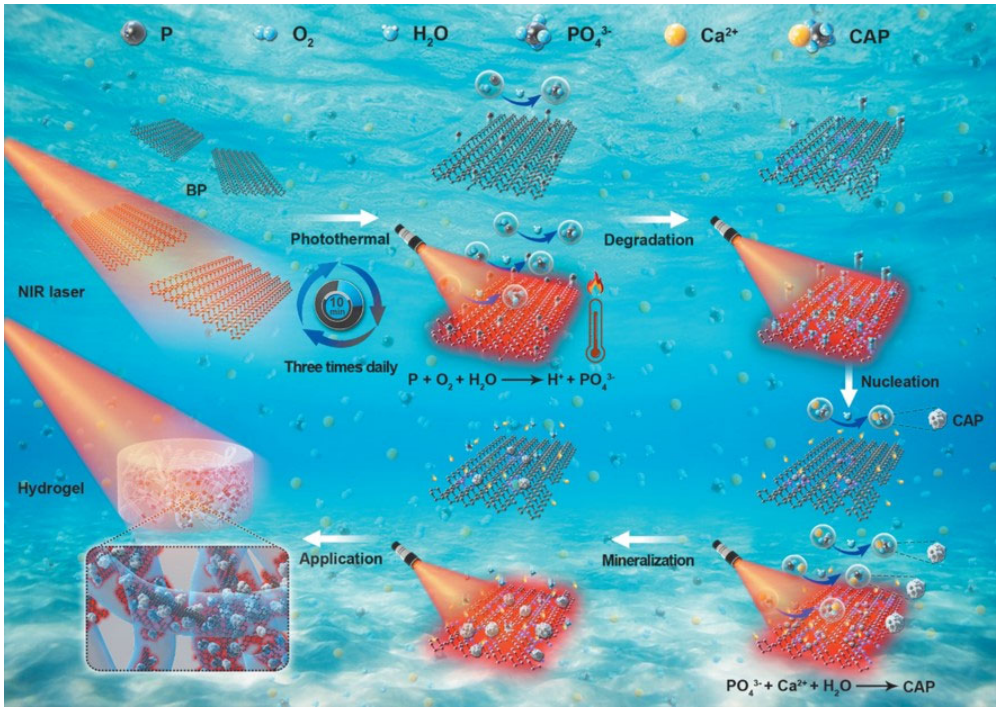

Figure 4. Mechanism of in situ mineralization of BP/agarose hydrogels under NIR irradiation [124]. Copyright 2020, Wiley.

Sanchez et al. fabricated a fibrin/GNPs hydrogel and C3H-BMP-2^{high} cells were successfully entrapped within the hydrogels (the composite hydrogel was named NIR-BMP2-HG). Under the dual stimulation of heat treatment induced by NIR irradiation (42–43 °C) and rapamycin (Rm), C3H-BMP-2^{high} cells can secrete BMP-2 to promote bone regeneration, and when heat treatment or rapamycin was used alone, BMP-2 secretion was negligible (Figure 5). BMP-2 is involved in the differentiation of BMSCs into osteoblasts and promotes the migration of BMSCs to the defect area [127,128]. The mild photothermal hydrogel increased the expression of heat shock proteins (HSP). Moreover, HSP70 can enhance the heat resistance of cells, and HSP47 promotes the maturation of osteogenic COL I. These two types of HSPs can promote cell osteogenic activity. Meanwhile, Ma et al. recently demonstrated that NIR irradiation + nHA could promote the expression of HSP47 and HSP70 [129].

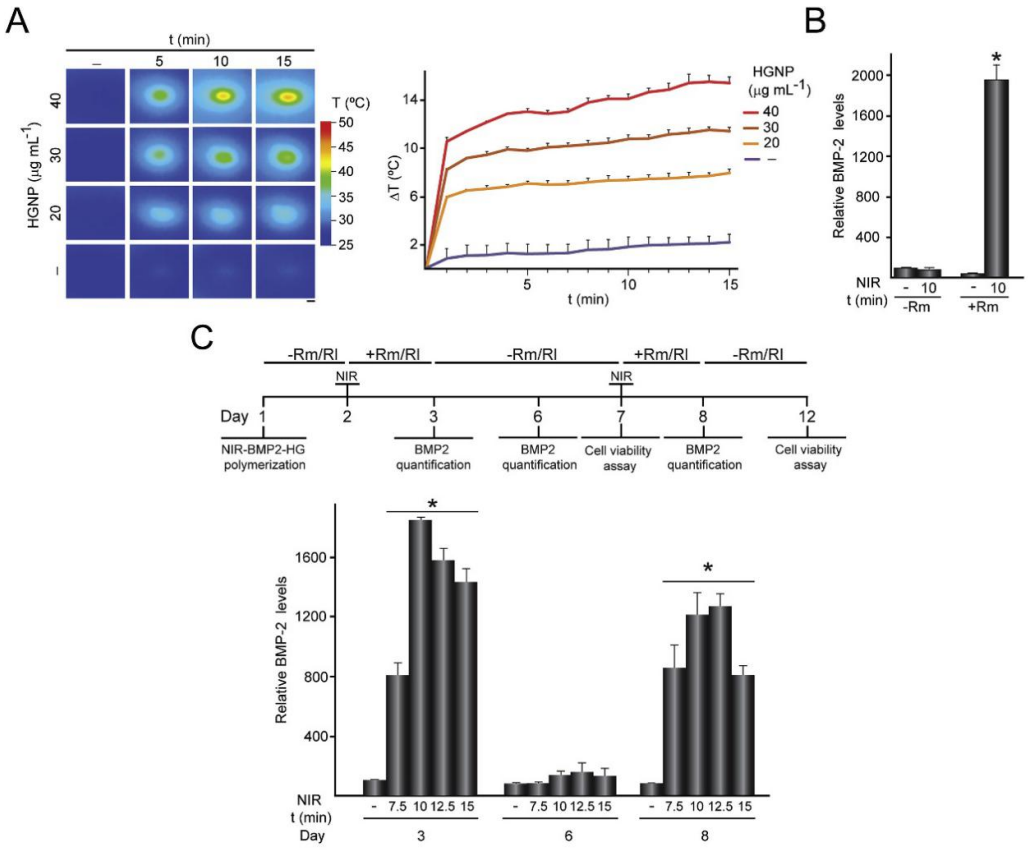

Figure 5. Activation of NIR-BMP-2-HG triggered by NIR light. (**A**) NIR-BMP-2-HG, polymerized with the indicated concentration of HGNP, were cultured for 1 day and then irradiated with NIR laser for the indicated times. (**B**) BMP-2 concentration in media conditioned by NIR-BMP-2-HG polymerized with 30 μg·mL^{-1} HGNP. (**C**) NIR-BMP-2-HG, polymerized with 30 μg·mL^{-1} HGNP, were NIR-irradiated in the presence of 10 nM Rm or 100 nM rapalog AP21967 (Rl). Timeline scheme of NIR-BMP-2-HG preparation, NIR irradiation of hydrogel (NIR), * $p < 0.05$, culture in the absence (-Rm/Rl) or presence (+Rm/Rl) of rapamycin or rapalog and analytical assays [127]. Copyright 2020, Elsevier.

4. Photothermal Hydrogels in Wound Healing and Bone Repair

For wound healing and bone repair, control of infection, cell proliferation, and angiogenesis are both key factors. The hydrogel can mimic the extracellular matrix in defect areas and provide a microenvironment for tissue regeneration. Further, the photothermal conversion ability of hybrid hydrogels play an important role in wound healing and bone repair. Mild heat (41 °C–43 °C) can promote cell proliferation, increase blood flow, and further induce tissue regeneration. Hyperthermia (>50 °C) can denature proteins, destroy the integrity of cell membranes, and inhibit the growth of bacteria. Therefore, photothermal hydrogels could be applied in various medical applications to treat infection and promote tissue regeneration. Table 1 summarizes the applications of hydrogels with PTT in wound healing and bone engineering.

Table 1. Hydrogels with PTT for wound healing and bone engineering.

Hydrogels	Photothermal Agents	Concentration	Intensity and Time	Temperature	Application	Reference
NOCS/OSA/FA	FA(Fe_2SiO_4)	5 mg/mL	0.36 W/cm^2 10 min	40 °C	Ion release Angiogenesis	[112]
CMCS/OSA/CuS	CuS	0.8 mg/mL	1 W/cm^2 5 min	50 °C	Antibacterial Angiogenesis	[103]
CuS/HA	CuS	0.2 mg/mL	1 W/cm^2	53.1 °C	Wound healing	[115]

			10 min		Angiogenesis	
NIPAAm/ AAm/CuS/ mSiO2	CuS/mSiO$_2$ NPs	1.5 mg/mL	2 W/cm^2 8 min	59.5 °C	Antibacterial effect	[113]
GelMA/BP	BP	1 mg/mL	1 W/cm^2 5 min	55.3 °C	Antibacterial effect Bone regeneration	[125]
BP/CS/PRP	BP	0.05 mg/mL	1 W/cm^2 8 min	45 °C	Drug release Antiarthritic	[130]
PDA/GC/Cip	PDA NPs	4 mg/mL	0.5 W/cm^2 10 min	46.8 °C	Antibacterial effect Drug release	[131]
Gel-PDA/Cur	PDA/Cur	2 mg/mL	1 W/cm^2 10 min	50.9 °C	Antibacterial effect Drug release	[95]
MPDA/GO/ CNF	MPDA/GO	10 mg/mL	2 W/cm^2 10 min	56 °C	Drug release	[90]
GelMA/oDex/BN N6@ZIF8/ PDA	PDA/ZIF8	1 mg/mL	2 W/cm^2 10 min	50 °C	Antibacterial effect Angiogenesis	[121]

4.1. Wound Healing

Common clinical traumas are caused by fractures, tumors, diabetes, etc., and are often accompanied by serious infections. To promote wound healing, many dressings have been developed to control infection, promote hemostasis, and improve angiogenesis [132–134]. The development of hydrogel with excellent antibacterial properties, good compatibility, and degradable ability is a promising strategy for wound healing [135,136]. Hydrogels with a photothermal conversion ability can regulate the temperature by changing the NIR irradiation intensity/time, photothermal initiator concentration/ratio, and cycling time [137,138]. Hyperthermia (>50 °C) can effectively inhibit bacterial growth, and mild heat (41 °C–43 °C) accelerates wound closure. For example, GelMA/BACA–Cu NPs hydrogels were prepared and possess good photothermal ability under laser exposure. After 10 min of NIR irradiation, the hyperthermia (>55 °C) of hydrogels can effectively inhibit the proliferation of bacteria, and Cu^{2+} played an antibacterial role with co-therapy of bacteria [139]. After 14 days, the wound closure rate of NIR+ GelMA/BACA–Cu NPs hydrogel group was 95.1%, while the control group showed a lower closure rate of about 79.3% [68]. Zhou et al. recently fabricated an oxidized dextran/PEG/CuS hydrogel and found that it played an important role in accelerating angiogenesis and promoting the proliferation of fibroblasts [140].

Francisco et al. recently demonstrated that the CuS NP/fibrinogen hydrogel increased the capillary density compared to the control group, suggesting that Cu^{2+} can promote angiogenesis [141]. Huang et al. expounded that the GelMA/GO-βCD-BNN6 hydrogel could achieve the controlled release of NO under NIR irradiation. Hyperthermia (about 60 °C) and the NO released (4 μM) provided excellent antibacterial properties in vitro/vivo [82]. Moreover, the GelMA/oDex/BZP (BNN6/ZIF8/PDA) hydrogel showed NIR-irradiation dependent NO release. Figure 6 shows that the Gel+NIR group could accelerate wound healing. Masson's trichrome staining and hematoxylin and eosin demonstrated that Gel+NIR group can effectively reduce tissue inflammation and accelerate the regeneration of skin appendages [121].

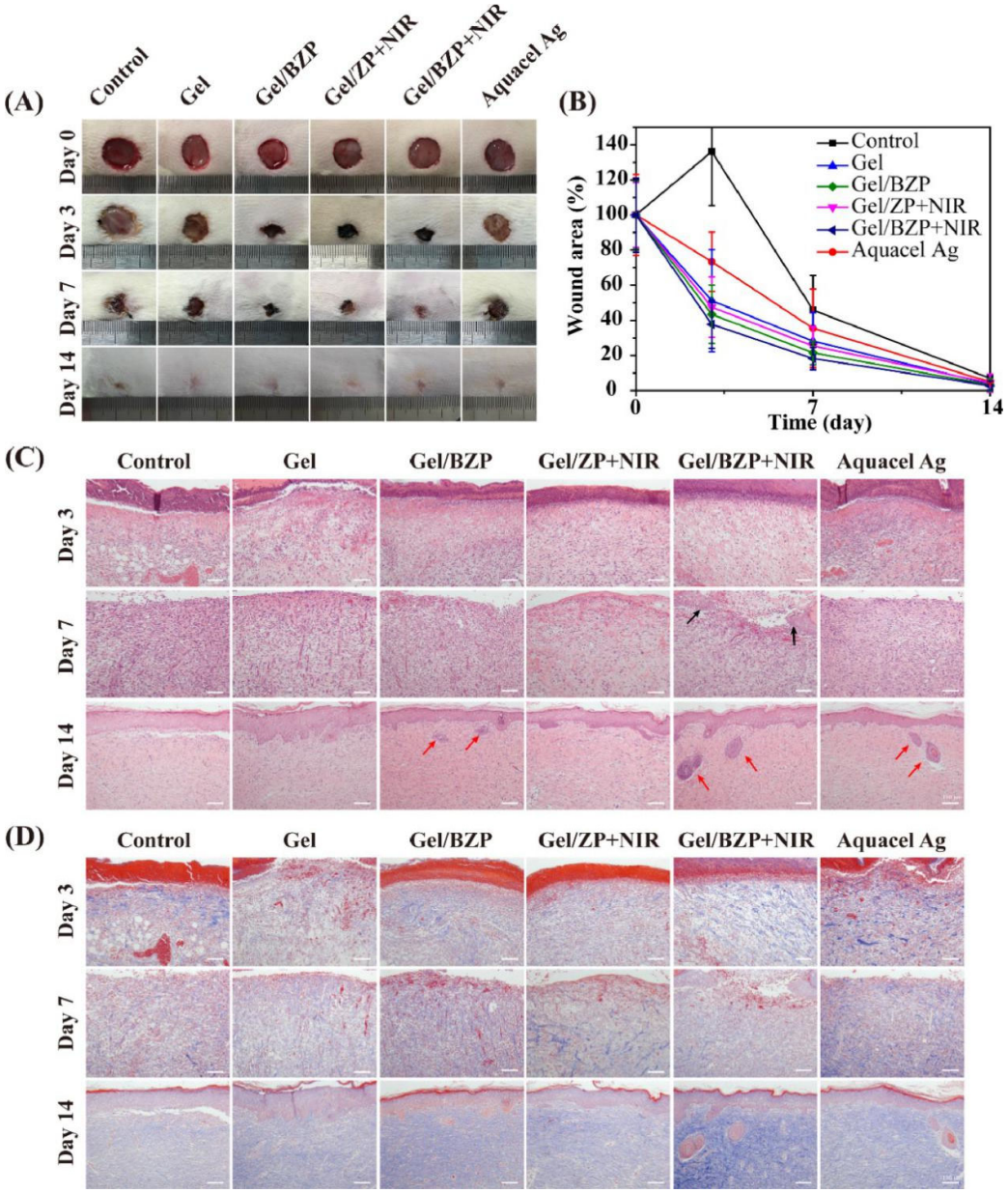

Figure 6. In vivo animal experiment assessment of hydrogels for wound healing. (**A**) Images of wounds treated with different hydrogels on 0, 3, 7, and 14 d. (**B**) Wound area values at different healing times. (**C**) H&E staining and (**D**) Masson's trichrome staining of the wound section at 3, 7, and 14 d; scale bar = 100 μm.(ZP: ZIF8/PDA, BZP: BNN6/ZIF8/PDA) [121]. Copyright 2020, Elsevier.

The effective control of inflammation is another key to wound healing. Sun et al. demonstrated that PEG/PDA hydrogel can effectively reduce the inflammatory response in methicillin-resistant *Staphylococcus aureus*-infected rats and accelerate wound healing [142]. Chu et al. recently developed a biomaterial with Cu-carbon dots + NIR and the wound closure rate reached 96% after treatments for 14 days, while the wound healing rate of the control group was 62%. Hematoxylin and eosin staining in the Cu-carbon dots + NIR group showed more neovascularization, collagen deposition, and re-epithelization than that in the control group [143].

Hyperthermia induced by NIR irradiation has a short-term antibacterial effect. When the NIR irradiation is stopped, the remaining bacteria cannot be effectively inhibited. To

strengthen the antibacterial property of hydrogels, some studies have developed hydrogels loaded with antibacterial drugs for co-therapy [137]. Furthermore, NIR-triggered drug release had been successfully achieved. Ciprofloxacin (Cip) was loaded on PDA via π−π stacking and hydrogen bonds, which was released rapidly under NIR irradiation. The PDA NP-Cip+NIR group showed excellent inhibition of bacterial activity (2.1×10^6 CFU/g) compared to the control group (6.0×10^6 CFU/g) [131]. Deng et al. successfully fabricated a polysaccharide hydrogel embedded with ferric tannate (TA-Fe) nanoparticles and vancomycin. Under NIR irradiation, the vancomycin was released explosively. After the NIR was removed, a small amount of the vancomycin was released continuously. After 5 days of treatment, the Gel/vancomycin+NIR group showed the highest wound closure rate (80%) and erythema and edema were not observed [144].

Interestingly, the proliferation of bacteria often leads to a decrease in pH in the microenvironment. When the environment changes from an acidic to a neutral condition, the color of bromothymol blue (BTB), a pH-sensitive reagent, changed from yellow to green. Hence, Wang et al. designed a visual photothermal treatment strategy for infectious subcutaneous defects based on BTB. They employed PTDBD as a photo-initiator, β-glycerophosphate as a sol-gel conversion agent, and chitosan as scaffold material to obtain a visual antibacterial hydrogel. After 8 min of NIR irradiation, the temperature of the hydrogel up to 55 °C and showed a strong destructive effect on S. aureus [145,146].

4.2. Bone Regeneration

Bone defect repair usually requires the proliferation and differentiation of BMSCs, angiogenesis, and the deposition of calcifications. However, common clinical bone defect treatment, such as that for open fractures, are often accompanied by severe infection and tissue ischemic necrosis. As a reusable, nontoxic, and noninvasive new treatment strategy, local heat induced by PTT has shown excellent osteogenesis ability in vitro/vivo. The excellent biocompatibility, adjustable degradability, and porous structure of hydrogels can reduce the inflammatory response produced by implant materials and provide scaffolds for new bone-growth [147]. When hydrogels with PTT is applied to repair bone defects, it is divided into the following stages: (1) controlling infection to alleviate inflammation; (2) neovascularization to supply nutrients and oxygen; (3) promoting the proliferation and differentiation of BMSCs into osteoblasts to migrate toward the defect area; and (4) promoting calcification deposition and new bone formation.

Bone defects often require the implantation of artificial materials to promote bone regeneration, but irregular bone surfaces and implant materials may cause bacterial colonization and induce serious infections. Hyperthermia induced by PTT inhibits the growth of bacteria and may cause irreversible damage to normal cells [148]. Hence, researchers generally added antibacterial substances such as Cu^{2+} into the hydrogel to improve antibacterial properties. Heat (about 46 °C) induced by gold nanoparticles under NIR irradiation could stimulate BMP-2 expression in bone defect cells and promote the mineralization of new bone [149].

Recently research indicated that the incorporation of photothermal agents can enhance the osteogenic properties of hydrogels. BP/platelet-rich plasma (PRP)-chitosan hydrogel can effectively destroy diseased tissues such as rheumatoid arthritis through photothermal conversion and generate reactive oxygen species under NIR irradiation. PRP could improve the adhesion of BMSCs on the surface of the hydrogel. Then PO_4^{3-} produced by degradation can form CaP by in situ biomineralization with Ca^{2+} to enhance the osteogenesis process [130]. Luo et al. recently demonstrated that an oxidized sodium alginate/CS/PDA/nHA hydrogel showed high osteogenic ability because of the adhesion ability of PDA. In the long-term bone regeneration process, osteoblasts gradually proliferated, differentiated, and migrated to the defect area [150].

Previous research demonstrated that a single NIR irradiation has no significant effect on osteoblast proliferation. Periodic and long-term local mild heat stimulation can upregulate the expression of osteoblast-related genes. Xue et al. recently found that with a

BGN/PDA/fibrin glue hydrogel and MC3T3-E1 cells co-cultured for 3 days with 10 min of NIR irradiation, there was negligible difference in MC3T3-E1 cells with and without NIR irradiation [151]. Compared to a single NIR irradiation, Ma et al. demonstrated that nHA/GO/CS scaffolds cultured with MC3T3-E1 cells (42 ± 0.5 °C for 60 s for 3 d) could significantly promote cell proliferation [129]. Zhang et al. also found a significant increase in cell proliferation on HA/graphene/CS scaffolds cultured with MC3T3-E1 cells (under NIR irradiation for 3 min to 43 °C for 3 days) [152]. This evidence suggests the necessity of periodic thermal stimulation in promoting osteogenesis.

To bone regeneration, the microenvironment regulated by signal molecules, such as parathyroid hormone (PTH), is crucial. However, unpredictable drug distribution and suboptimal local concentration limit its therapeutic effect. Wang et al. recently fabricated a CS/rGO hydrogel film and successfully loaded with teriparatide (PTH 1–34, an FDA-approved drug for osteoporosis treatment), which achieved pulsed release under NIR irradiation. In the osteoporotic rat model of bone defect, the local pulsatile teriparatide release group showed a higher ratio of new bone formation (BV/TV: 22.80%) than the control group (BV/TV 4.51%) (Figure 7) [153].

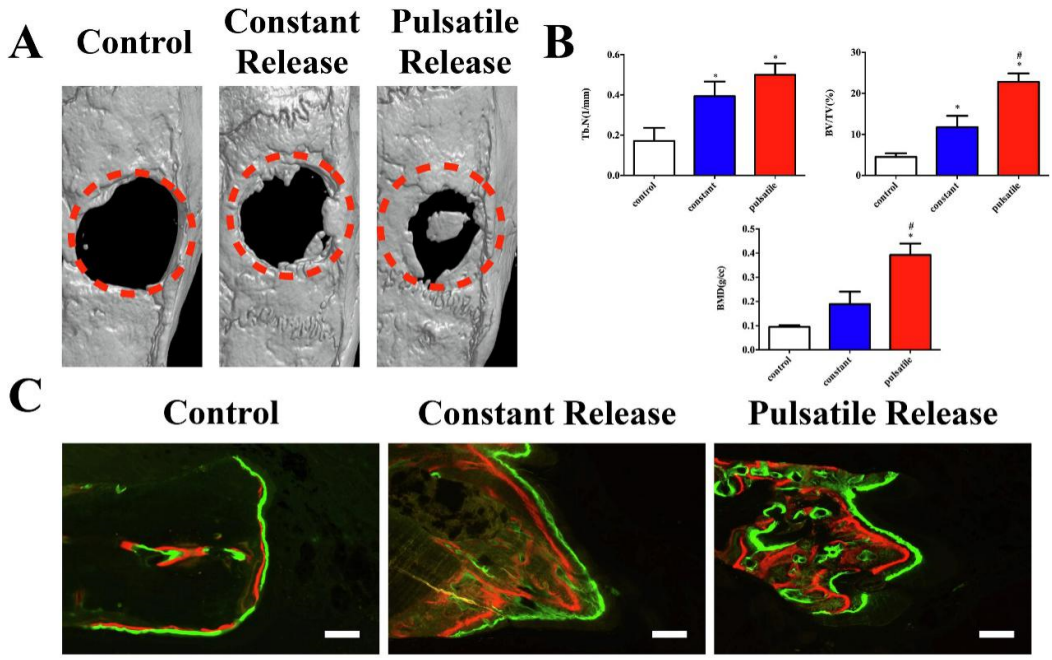

Figure 7. Micro-CT scanning and sequential fluorescent labeling. (**A**) Representative 3D reconstruction of the 4 mm calvarial defect from each group; (**B**) quantitative comparison of Tb.N, BV/TV and BMD among the control, constant release and pulsatile release groups. (**C**) Sequential fluorescent labeling of alizarin red (red) and calcein (green) represented the bone formation at 3 and 6 weeks. * $p < 0.05$ compared to the control group, # $p < 0.05$ compared to the constant release group. Scale bar = 20 μm [153]. Copyright 2021, Elsevier.

Moreover, some studies have reported a new hemicyanine dye LET-3 that can promote osteogenesis and realize photoacoustic imaging. LET-3 can be anchored on a calcium silicate scaffold, and further improve the expression of ALP. Especially, under NIR irradiation, higher ALP activity could induce a stronger photoacoustic effect. Hence, it is worth exploring to realize the noninvasive dynamic monitoring of osteogenesis in vivo through photoacoustic effect [154]. From this, researchers can design hydrogels with photothermal effects to promote osteogenesis and observe the process of osteogenesis using noninvasive imaging.

5. Prospective and Conclusion

Hydrogels with photothermal effects have gained increasing attention and are applied widely in wound healing and bone regeneration. It is one of the research hotspots in recent years to take advantage of the NIR absorption properties to achieve the target temperature. Besides, hyperthermia can be used for antibacterial and antitumor therapy, as mild local heat can simulate the hot spring effect to promote cell proliferation and accelerate wound healing. NIR-induced fluorescence imaging can also be used to track the development of bone regeneration dynamically and noninvasively. Remarkably, high temperature generated by photothermal materials under NIR irradiation, self-disinfecting personal protective equipment, as face masks, can be developed to fight COVID-19. This may be a promising strategy for the development of photothermal materials.

However, the low tissue penetration rate of NIR limits the application of PTT in deep tissue diseases. Besides, some materials have both photothermal conversion properties and magnetothermal conversion ability. To control drug release, photothermal-trigger release, pH-trigger release, and magnetothermal-trigger release are the key directions for future development.

In conclusion, hydrogels with PTT have excellent antibacterial effects and can promote tissue repair. In the future, researchers can make full use of the advantages of PTT to incorporate it in other treatment methods to overcome shortcomings, broaden applications, improve curative effects, and reduce costs. These advantages of PTT and hydrogels provide a new strategy in wound healing and bone tissue engineering.

Author Contributions: Conceptualization, X.Z., J.L.; methodology, X.Z., B.T., Y.W., M.Z., J.L.; writing—original draft preparation, X.Z.; writing—review and editing, J.L.; supervision, J.L.; project administration, J.L.; funding acquisition, J.L. All authors have read and agreed to the published version of the manuscript.

Funding: This research was financially funded by the National Natural Science Foundation (31972925), Sichuan Science and Technology Program (2020YJ0065).

Institutional Review Board Statement: Not applicable.

Informed Consent Statement: Not applicable.

Data Availability Statement: The data presented in this study are available on request from the corresponding author.

Acknowledgments: This work was financially supported by the National Natural Science Foundation (31972925), Sichuan Science and Technology Program (2020YJ0065).

Conflicts of Interest: The authors declare no conflict of interest.

References

1. Tao, N.; Liu, Y.; Wu, Y.; Li, X.; Li, J.; Sun, X.; Chen, S.; Liu, Y.-N. Minimally Invasive Antitumor Therapy Using Biodegradable Nanocomposite Micellar Hydrogel with Functionalities of NIR-II Photothermal Ablation and Vascular Disruption. *ACS Appl. Bio Mater.* **2020**, *3*, 4531–4542, doi:10.1021/acsabm.0c00465.
2. Cahill, S.V.; Kwon, H.; Back, J.; Lee, I.; Lee, S.; Alder, K.D.; Hao, Z.; Yu, K.E.; Dussik, C.M.; Kyriakides, T.R.; et al. Locally delivered adjuvant biofilm-penetrating antibiotics rescue impaired endochondral fracture healing caused by MRSA infection. *J. Orthop. Res.* **2021**, *39*, 402–414, doi:10.1002/jor.24965.
3. Contardi, M.; Kossyvaki, D.; Picone, P.; Summa, M.; Guo, X.; Heredia-Guerrero, J.A.; Giacomazza, D.; Carzino, R.; Goldoni, L.; Scoponi, G.; et al. Electrospun polyvinylpyrrolidone (PVP) hydrogels containing hydroxycinnamic acid derivatives as potential wound dressings. *Chem. Eng. J.* **2021**, *409*, 128144, doi:10.1016/j.cej.2020.128144.
4. Ahmed, R.; Afreen, A.; Tariq, M.; Zahid, A.A.; Masoud, M.S.; Ahmed, M.; Ali, I.; Akram, Z.; Hasan, A. Bone marrow mesenchymal stem cells preconditioned with nitric-oxide-releasing chitosan/PVA hydrogel accelerate diabetic wound healing in rabbits. *Biomed. Mater.* **2021**, *16*, 035014, doi:10.1088/1748-605x/abc28b.
5. Zhang, B.; He, J.; Shi, M.; Liang, Y.; Guo, B. Injectable self-healing supramolecular hydrogels with conductivity and photothermal antibacterial activity to enhance complete skin regeneration. *Chem. Eng. J.* **2020**, *400*, 125994, doi:10.1016/j.cej.2020.125994.
6. Gao, Y.; Du, H.; Xie, Z.; Li, M.; Zhu, J.; Xu, J.; Zhang, L.; Tao, J.; Zhu, J. Self-adhesive photothermal hydrogel films for solar-light assisted wound healing. *J. Mater. Chem. B* **2019**, *7*, 3644–3651, doi:10.1039/c9tb00481e.

7. Zhang, K.; Bai, X.; Yuan, Z.; Cao, X.; Jiao, X.; Li, Y.; Qin, Y.; Wen, Y.; Zhang, X. Layered nanofiber sponge with an improved capacity for promoting blood coagulation and wound healing. *Biomaterials* **2019**, *204*, 70–79, doi:10.1016/j.biomaterials.2019.03.008.
8. Qiu, G.; Huang, M.; Liu, J.; Wang, P.; Schneider, A.; Ren, K.; Oates, T.W.; Weir, M.D.; Xu, H.H.K.; Zhao, L. Antibacterial calcium phosphate cement with human periodontal ligament stem cell-microbeads to enhance bone regeneration and combat infection. *J. Tissue Eng. Regen. Med.* **2021**, *15*, 232–243, doi:10.1002/term.3169.
9. Zhang, X.; Chen, G.; Sun, L.; Ye, F.; Shen, X.; Zhao, Y. Claw-inspired microneedle patches with liquid metal encapsulation for accelerating incisional wound healing. *Chem. Eng. J.* **2021**, *406*, 126741, doi:10.1016/j.cej.2020.126741.
10. Wang, C.; Huang, W.; Zhou, Y.; He, L.; He, Z.; Chen, Z.; He, X.; Tian, S.; Liao, J.; Lu, B.; et al. 3D printing of bone tissue engineering scaffolds. *Bioact. Mater.* **2020**, *5*, 82–91, doi:10.1016/j.bioactmat.2020.01.004.
11. Yang, B.; Song, J.; Jiang, Y.; Li, M.; Wei, J.; Qin, J.; Peng, W.; Lasaosa, F.L.; He, Y.; Mao, H.; et al. Injectable Adhesive Self-Healing Multicross-Linked Double-Network Hydrogel Facilitates Full-Thickness Skin Wound Healing. *ACS Appl. Mater. Interfaces* **2020**, *12*, 57782–57797, doi:10.1021/acsami.0c18948.
12. Zhang, H.; Zheng, S.; Chen, C.; Zhang, D. A graphene hybrid supramolecular hydrogel with high stretchability, self-healable and photothermally responsive properties for wound healing. *RSC Adv.* **2021**, *11*, 6367–6373, doi:10.1039/d0ra09106e.
13. Liu, W.; Jing, X.; Xu, Z.; Teng, C. PEGDA/HA mineralized hydrogel loaded with Exendin4 promotes bone regeneration in rat models with bone defects by inducing osteogenesis. *J. Biomater. Appl.* **2021**, *35*, 1337–1346, doi:10.1177/0885328220987046.
14. Zhao, J.; Zhou, C.; Wu, C.; Wu, H.; Zhu, C.; Ye, C.; Wang, S.; Zou, D. Fe^{3+}-Induced Synchronous Formation of Composite Hydrogels for Effective Synergistic Tumor Therapy in NIR-I/II Biowindows. *ACS Appl. Mater. Interfaces* **2018**, *10*, 41947–41955, doi:10.1021/acsami.8b14649.
15. Chen, C.; Yang, X.; Li, S.-J.; Zhang, C.; Ma, Y.-N.; Gao, P.; Gao, S.-Z.; Huang, X.-J. Tannic acid–thioctic acid hydrogel: A novel injectable supramolecular adhesive gel for wound healing. *Green Chem.* **2021**, *23*, 1794–1804, doi:10.1039/d0gc02909b.
16. Zhang, S.; Xu, B.; Lu, X.; Wang, L.; Li, Y.; Ma, N.; Wei, H.; Zhang, X.; Wang, G. Readily producing a Silly Putty-like hydrogel with good self-healing, conductive and photothermal conversion properties based on dynamic coordinate bonds and hydrogen bonds. *J. Mater. Chem. C* **2020**, *8*, 6763–6770, doi:10.1039/d0tc00814a.
17. Gao, Q.; Hu, J.; Shi, J.; Wu, W.; Debeli, D.K.; Pan, P.; Shan, G. Fast photothermal poly(NIPAM-co-β-cyclodextrin) supramolecular hydrogel with self-healing through host–guest interaction for intelligent light-controlled switches. *Soft Matter* **2020**, *16*, 10558–10566, doi:10.1039/d0sm01501f.
18. Guo, B.; Qu, J.; Zhao, X.; Zhang, M. Degradable conductive self-healing hydrogels based on dextran-graft-tetraaniline and N-carboxyethyl chitosan as injectable carriers for myoblast cell therapy and muscle regeneration. *Acta Biomater.* **2019**, *84*, 180–193, doi:10.1016/j.actbio.2018.12.008.
19. Zhang, M.; Deng, F.; Tang, L.; Wu, H.; Ni, Y.; Chen, L.; Huang, L.; Hu, X.; Lin, S.; Ding, C. Super-ductile, injectable, fast self-healing collagen-based hydrogels with multi-responsive and accelerated wound-repair properties. *Chem. Eng. J.* **2021**, *405*, 126756, doi:10.1016/j.cej.2020.126756.
20. Uman, S.; Dhand, A.; Burdick, J.A. Recent advances in shear-thinning and self-healing hydrogels for biomedical applications. *J. Appl. Polym. Sci.* **2020**, *137*, 137, doi:10.1002/app.48668.
21. Jiang, W.; Chen, Y.; Zhao, L.; Xu, J.; Zhao, R.; Serpe, M.J.; Hu, L. Bioinspired tissue-compliant hydrogels with multifunctions for synergistic surgery–photothermal therapy. *J. Mater. Chem. B* **2020**, *8*, 10117–10125, doi:10.1039/d0tb01907k.
22. Nakielski, P.; Pawłowska, S.; Rinoldi, C.; Ziai, Y.; De Sio, L.; Urbanek, O.; Zembrzycki, K.; Pruchniewski, M.; Lanzi, M.; Salatelli, E.; et al. Multifunctional Platform Based on Electrospun Nanofibers and Plasmonic Hydrogel: A Smart Nanostructured Pillow for Near-Infrared Light-Driven Biomedical Applications. *ACS Appl. Mater. Interfaces* **2020**, *12*, 54328–54342, doi:10.1021/acsami.0c13266.
23. Yang, Y.; Ma, L.; Cheng, C.; Deng, Y.; Huang, J.; Fan, X.; Nie, C.; Zhao, W.; Zhao, C. Nonchemotherapic and Robust Dual-Responsive Nanoagents with On-Demand Bacterial Trapping, Ablation, and Release for Efficient Wound Disinfection. *Adv. Funct. Mater.* **2018**, *28*, doi:10.1002/adfm.201705708.
24. Zhang, X.; He, Y.; Huang, P.; Jiang, G.; Zhang, M.; Yu, F.; Zhang, W.; Fu, G.; Wang, Y.; Li, W.; et al. A novel mineralized high strength hydrogel for enhancing cell adhesion and promoting skull bone regeneration in situ. *Compos. Part B Eng.* **2020**, *197*, 108183, doi:10.1016/j.compositesb.2020.108183.
25. Zhu, Y.; Deng, S.; Ma, Z.; Kong, L.; Li, H.; Chan, H.F. Macrophages activated by akermanite/alginate composite hydrogel stimulate migration of bone marrow-derived mesenchymal stem cells. *Biomed. Mater.* **2021**, *16*, 045004, doi:10.1088/1748-605x/abe80a.
26. Rehman, S.; Ranjha, N.M.; Raza, M.R.; Hanif, M.; Majed, A.; Ameer, N. Enteric-coated Ca-alginate hydrogel beads: A promising tool for colon targeted drug delivery system. *Polym. Bull.* **2020**, 1–15, doi:10.1007/s00289-020-03359-1.
27. Li, J.; Yu, F.; Chen, G.; Liu, J.; Li, X.-L.; Cheng, B.; Mo, X.-M.; Chen, C.; Pan, J.-F. Moist-Retaining, Self-Recoverable, Bioadhesive, and Transparent in Situ Forming Hydrogels to Accelerate Wound Healing. *ACS Appl. Mater. Interfaces* **2019**, *12*, 2023–2038, doi:10.1021/acsami.9b17180.
28. Ma, T.; Sheng, S.; Dong, X.; Zhang, Y.; Li, X.; Zhu, D.; Lv, F. A photo-triggered hydrogel for bidirectional regulation with imaging visualization. *Soft Matter* **2020**, *16*, 7598–7605, doi:10.1039/d0sm01156h.
29. Hou, L.; Shan, X.; Hao, L.; Feng, Q.; Zhang, Z. Copper sulfide nanoparticle-based localized drug delivery system as an effective cancer synergistic treatment and theranostic platform. *Acta Biomater.* **2017**, *54*, 307–320, doi:10.1016/j.actbio.2017.03.005.

30. Liu, B.; Sun, J.; Zhu, J.; Li, B.; Ma, C.; Gu, X.; Liu, K.; Zhang, H.; Wang, F.; Su, J.; et al. Injectable and NIR-Responsive DNA–Inorganic Hybrid Hydrogels with Outstanding Photothermal Therapy. *Adv. Mater.* **2020**, *32*, doi:10.1002/adma.202004460.
31. Zhang, X.; Cheng, G.; Xing, X.; Liu, J.; Cheng, Y.; Ye, T.; Wang, Q.; Xiao, X.; Li, Z.; Deng, H. Near-Infrared Light-Triggered Porous AuPd Alloy Nanoparticles to Produce Mild Localized Heat to Accelerate Bone Regeneration. *J. Phys. Chem. Lett.* **2019**, *10*, 4185–4191, doi:10.1021/acs.jpclett.9b01735.
32. Su, J.; Lu, S.; Jiang, S.; Li, B.; Liu, B.; Sun, Q.; Li, J.; Wang, F.; Wei, Y. Engineered Protein Photo-Thermal Hydrogels for Outstanding In Situ Tongue Cancer Therapy. *Adv. Mater.* **2021**, *33*, 2100619, doi:10.1002/adma.202100619.
33. He, J.; Chen, G.; Zhao, P.; Ou, C. Near-infrared light-controllable bufalin delivery from a black phosphorus-hybrid supramolecular hydrogel for synergistic photothermal-chemo tumor therapy. *Nano Res.* **2021**, 1–11, doi:10.1007/s12274-021-3325-z.
34. Yao, Q.; Lan, Q.-H.; Jiang, X.; Du, C.-C.; Zhai, Y.-Y.; Shen, X.; Xu, H.-L.; Xiao, J.; Kou, L.; Zhao, Y.-Z. Bioinspired biliverdin/silk fibroin hydrogel for antiglioma photothermal therapy and wound healing. *Theranostics* **2020**, *10*, 11719–11736, doi:10.7150/thno.47682.
35. Hou, X.-L.; Dai, X.; Yang, J.; Zhang, B.; Zhao, D.-H.; Li, C.-Q.; Yin, Z.-Y.; Zhao, Y.-D.; Liu, B. Injectable polypeptide-engineered hydrogel depot for amplifying the anti-tumor immune effect induced by chemo-photothermal therapy. *J. Mater. Chem. B* **2020**, *8*, 8623–8633, doi:10.1039/d0tb01370f.
36. Pedersen, S.L.; Huynh, T.H.; Pöschko, P.; Fruergaard, A.S.; Olesen, M.T.J.; Chen, Y.; Birkedal, H.; Subbiahdoss, G.; Reimhult, E.; Thøgersen, J.; et al. Remotely Triggered Liquefaction of Hydrogel Materials. *ACS Nano* **2020**, *14*, 9145–9155, doi:10.1021/acsnano.0c04522.
37. Shao, J.; Ruan, C.; Xie, H.; Li, Z.; Wang, H.; Chu, P.K.; Yu, X.-F. Black-Phosphorus-Incorporated Hydrogel as a Sprayable and Biodegradable Photothermal Platform for Postsurgical Treatment of Cancer. *Adv. Sci.* **2018**, *5*, 1700848, doi:10.1002/advs.201700848.
38. Guan, G.; Win, K.Y.; Yao, X.; Yang, W.; Han, M. Plasmonically Modulated Gold Nanostructures for Photothermal Ablation of Bacteria. *Adv. Healthc. Mater.* **2021**, *10*, e2001158, doi:10.1002/adhm.202001158.
39. Li, B.; Zhang, L.; Zhang, Z.; Gao, R.; Li, H.; Dong, Z.; Wang, Q.; Zhou, Q.; Wang, Y. Physiologically stable F127-GO supramolecular hydrogel with sustained drug release characteristic for chemotherapy and photothermal therapy. *RSC Adv.* **2018**, *8*, 1693–1699, doi:10.1039/c7ra12099k.
40. Nowroozi, N.; Faraji, S.; Nouralishahi, A.; Shahrousvand, M. Biological and structural properties of graphene oxide/curcumin nanocomposite incorporated chitosan as a scaffold for wound healing application. *Life Sci.* **2021**, *264*, 118640, doi:10.1016/j.lfs.2020.118640.
41. Huang, L.; Zhou, J.; Chen, Y.; Li, W.; Han, X.; Wang, L. Engineering Microcapsules for Simultaneous Delivery of Combinational Therapeutics. *Adv. Mater. Technol.* **2020**, *5*, 5, doi:10.1002/admt.202000623.
42. Zhang, L.; Ren, S.; Chen, C.; Wang, D.; Liu, B.; Cai, D.; Wu, Z. Near infrared light-driven release of pesticide with magnetic collectability using gel-based nanocomposite. *Chem. Eng. J.* **2021**, *411*, 127881, doi:10.1016/j.cej.2020.127881.
43. Li, L.; Fu, L.; Ai, X.; Zhang, J.; Zhou, J. Design and Fabrication of Temperature-Sensitive Nanogels with Controlled Drug Release Properties for Enhanced Photothermal Sterilization. *Chem. A Eur. J.* **2017**, *23*, 18180–18186, doi:10.1002/chem.201702796.
44. Shou, X.; Liu, Y.; Wu, D.; Zhang, H.; Zhao, Y.; Sun, W.; Shen, X. Black phosphorus quantum dots doped multifunctional hydrogel particles for cancer immunotherapy. *Chem. Eng. J.* **2020**, *408*, 127349, doi:10.1016/j.cej.2020.127349.
45. Han, X.-M.; Zheng, K.-W.; Wang, R.-L.; Yue, S.-F.; Chen, J.; Zhao, Z.-W.; Song, F.; Su, Y.; Ma, Q. Functionalization and optimization-strategy of graphene oxide-based nanomaterials for gene and drug delivery. *Am. J. Transl. Res.* **2020**, *12*, 1515–1534.
46. Fan, L.; Zhang, X.; Liu, X.; Sun, B.; Li, L.; Zhao, Y. Responsive Hydrogel Microcarrier-Integrated Microneedles for Versatile and Controllable Drug Delivery. *Adv. Healthc. Mater.* **2021**, *10*, 2002249, doi:10.1002/adhm.202002249.
47. GhavamiNejad, A.; Samarikhalaj, M.; Aguilar, L.E.; Park, C.H.; Kim, C.S. pH/NIR Light-Controlled Multidrug Release via a Mussel-Inspired Nanocomposite Hydrogel for Chemo-Photothermal Cancer Therapy. *Sci. Rep.* **2016**, *6*, 33594, doi:10.1038/srep33594.
48. Dong, M.; Shi, B.; Liu, D.; Liu, J.-H.; Zhao, D.; Yu, Z.-H.; Shen, X.-Q.; Gan, J.-M.; Shi, B.-L.; Qiu, Y.; et al. Conductive Hydrogel for a Photothermal-Responsive Stretchable Artificial Nerve and Coalescing with a Damaged Peripheral Nerve. *ACS Nano* **2020**, *14*, 16565–16575, doi:10.1021/acsnano.0c05197.
49. He, J.; Shi, M.; Liang, Y.; Guo, B. Conductive adhesive self-healing nanocomposite hydrogel wound dressing for photothermal therapy of infected full-thickness skin wounds. *Chem. Eng. J.* **2020**, *394*, 124888, doi:10.1016/j.cej.2020.124888.
50. Li, B.; Harlepp, S.; Gensbittel, V.; Wells, C.; Bringel, O.; Goetz, J.; Begin-Colin, S.; Tasso, M.; Begin, D.; Mertz, D. Near infra-red light responsive carbon nanotubes@mesoporous silica for photothermia and drug delivery to cancer cells. *Mater. Today Chem.* **2020**, *17*, 100308, doi:10.1016/j.mtchem.2020.100308.
51. Deng, Z.; Hu, T.; Lei, Q.; He, J.; Ma, P.X.; Guo, B. Stimuli-Responsive Conductive Nanocomposite Hydrogels with High Stretchability, Self-Healing, Adhesiveness, and 3D Printability for Human Motion Sensing. *ACS Appl. Mater. Interfaces* **2019**, *11*, 6796–6808, doi:10.1021/acsami.8b20178.
52. Lima-Sousa, R.; de Melo-Diogo, D.; Alves, C.G.; Cabral, C.S.; Miguel, S.P.; Mendonça, A.G.; Correia, I.J. Injectable in situ forming thermo-responsive graphene based hydrogels for cancer chemo-photothermal therapy and NIR light-enhanced antibacterial applications. *Mater. Sci. Eng. C* **2020**, *117*, 111294, doi:10.1016/j.msec.2020.111294.
53. Li, D.; Nie, W.; Chen, L.; McCoul, D.; Liu, D.; Zhang, X.; Ji, Y.; Yu, B.; He, C. Self-Assembled Hydroxyapatite-Graphene Scaffold for Photothermal Cancer Therapy and Bone Regeneration. *J. Biomed. Nanotechnol.* **2018**, *14*, 2003–2017, doi:10.1166/jbn.2018.2646.

54. Liao, J.; Shi, K.; Jia, Y.; Wu, Y.; Qian, Z. Gold nanorods and nanohydroxyapatite hybrid hydrogel for preventing bone tumor recurrence via postoperative photothermal therapy and bone regeneration promotion. *Bioact. Mater.* **2021**, *6*, 2221–2230, doi:10.1016/j.bioactmat.2021.01.006.
55. Matai, I.; Kaur, G.; Soni, S.; Sachdev, A.; Vikas; Mishra, S. Near-infrared stimulated hydrogel patch for photothermal therapeutics and thermoresponsive drug delivery. *J. Photochem. Photobiol. B Biol.* **2020**, *210*, 111960, doi:10.1016/j.jphotobiol.2020.111960.
56. Mirrahimi, M.; Beik, J.; Mirrahimi, M.; Alamzadeh, Z.; Teymouri, S.; Mahabadi, V.P.; Eslahi, N.; Tazehmahalleh, F.E.; Ghaznavi, H.; Shakeri-Zadeh, A.; et al. Triple combination of heat, drug and radiation using alginate hydrogel co-loaded with gold nanoparticles and cisplatin for locally synergistic cancer therapy. *Int. J. Biol. Macromol.* **2020**, *158*, 617–626, doi:10.1016/j.ijbiomac.2020.04.272.
57. Tong, L.; Liao, Q.; Zhao, Y.; Huang, H.; Gao, A.; Zhang, W.; Gao, X.; Wei, W.; Guan, M.; Chu, P.K.; et al. Near-infrared light control of bone regeneration with biodegradable photothermal osteoimplant. *Biomaterials* **2019**, *193*, 1–11, doi:10.1016/j.biomaterials.2018.12.008.
58. Xie, J.; Fan, T.; Kim, J.H.; Xu, Y.; Wang, Y.; Liang, W.; Qiao, L.; Wu, Z.; Liu, Q.; Hu, W.; et al. Emetine-Loaded Black Phosphorus Hydrogel Sensitizes Tumor to Photothermal Therapy through Inhibition of Stress Granule Formation. *Adv. Funct. Mater.* **2020**, *30*, doi:10.1002/adfm.202003891.
59. Liu, Y.; Li, F.; Guo, Z.; Xiao, Y.; Zhang, Y.; Sun, X.; Zhe, T.; Cao, Y.; Wang, L.; Lu, Q.; et al. Silver nanoparticle-embedded hydrogel as a photothermal platform for combating bacterial infections. *Chem. Eng. J.* **2020**, *382*, 122990, doi:10.1016/j.cej.2019.122990.
60. Zhang, W.; Gu, J.; Li, K.; Zhao, J.; Ma, H.; Wu, C.; Zhang, C.; Xie, Y.; Yang, F.; Zheng, X. A hydrogenated black TiO2 coating with excellent effects for photothermal therapy of bone tumor and bone regeneration. *Mater. Sci. Eng. C* **2019**, *102*, 458–470, doi:10.1016/j.msec.2019.04.025.
61. Wang, C.; Wang, X.; Dong, K.; Luo, J.; Zhang, Q.; Cheng, Y. Injectable and responsively degradable hydrogel for personalized photothermal therapy. *Biomaterials* **2016**, *104*, 129–137, doi:10.1016/j.biomaterials.2016.07.013.
62. Su, J.; Lu, S.; Hai, J.; Liang, K.; Li, T.; Sun, S.; Chen, F.; Yang, Z.; Wang, B. Confining Carbon Dots in Porous Wood: The Singlet Oxygen Enhancement Strategy for Photothermal Signal-Amplified Detection of Mn^{2+}. *ACS Sustain. Chem. Eng.* **2020**, *8*, 17687–17696, doi:10.1021/acssuschemeng.0c05352.
63. Cui, Q.; Yuan, H.; Bao, X.; Ma, G.; Wu, M.; Xing, C. Synergistic Photodynamic and Photothermal Antibacterial Therapy Based on a Conjugated Polymer Nanoparticle-Doped Hydrogel. *ACS Appl. Bio Mater.* **2020**, *3*, 4436–4443, doi:10.1021/acsabm.0c00423.
64. Lei, Z.; Zhu, W.; Xu, S.; Ding, J.; Wan, J.; Wu, P. Hydrophilic $MoSe_2$ Nanosheets as Effective Photothermal Therapy Agents and Their Application in Smart Devices. *ACS Appl. Mater. Interfaces* **2016**, *8*, 20900–20908, doi:10.1021/acsami.6b07326.
65. Liu, B.; Gu, X.; Sun, Q.; Jiang, S.; Sun, J.; Liu, K.; Wang, F.; Wei, Y. Injectable In Situ Induced Robust Hydrogel for Photothermal Therapy and Bone Fracture Repair. *Adv. Funct. Mater.* **2021**, *31*, 2010779, doi:10.1002/adfm.202010779.
66. Liu, Y.; Xiao, Y.; Cao, Y.; Guo, Z.; Li, F.; Wang, L. Construction of Chitosan-Based Hydrogel Incorporated with Antimonene Nanosheets for Rapid Capture and Elimination of Bacteria. *Adv. Funct. Mater.* **2020**, *30*, doi:10.1002/adfm.202003196.
67. Li, Q.; Wen, J.; Liu, C.; Jia, Y.; Wu, Y.; Shan, Y.; Qian, Z.; Liao, J. Graphene-Nanoparticle-Based Self-Healing Hydrogel in Preventing Postoperative Recurrence of Breast Cancer. *ACS Biomater. Sci. Eng.* **2019**, *5*, 768–779, doi:10.1021/acsbiomaterials.8b01475.
68. Tao, B.; Lin, C.; Deng, Y.; Yuan, Z.; Shen, X.; Chen, M.; He, Y.; Peng, Z.; Hu, Y.; Cai, K. Copper-nanoparticle-embedded hydrogel for killing bacteria and promoting wound healing with photothermal therapy. *J. Mater. Chem. B* **2019**, *7*, 2534–2548, doi:10.1039/c8tb03272f.
69. Tong, C.; Zhong, X.; Yang, Y.; Liuc, X.; Zhonga, G.; Xiaoa, C.; Liuad, B.; Wangc, W.; Yangb, X. PB@PDA@Ag nanosystem for synergistically eradicating MRSA and accelerating diabetic wound healing assisted with laser irradiation. *Biomaterials* **2020**, *243*, 119936, doi:10.1016/j.biomaterials.2020.119936.
70. Tan, B.; Huang, L.; Wu, Y.; Liao, J. Advances and trends of hydrogel therapy platform in localized tumor treatment: A review. *J. Biomed. Mater. Res. Part A* **2021**, *109*, 404–425, doi:10.1002/jbm.a.37062.
71. Homsirikamol, C.; Suvanasuthi, S.; Viravaidya-Pasuwat, K. Inclusion of IR-820 into Soybean-Phosphatides-Based Nanoparticles for Near-Infrared-Triggered Release and Endolysosomal Escape in HaCaT Keratinocytes at Insignificant Cytotoxic Level. *Int. J. Nanomed.* **2020**, *15*, 8717–8737, doi:10.2147/ijn.s267119.
72. Dong, X.; Liang, J.; Yang, A.; Qian, Z.; Kong, D.; Lv, F. Fluorescence imaging guided CpG nanoparticles-loaded IR820-hydrogel for synergistic photothermal immunotherapy. *Biomaterials* **2019**, *209*, 111–125, doi:10.1016/j.biomaterials.2019.04.024.
73. Wang, K.; Zhang, Y.; Wang, J.; Yuan, A.; Sun, M.; Wu, J.; Hu, Y. Self-assembled IR780-loaded transferrin nanoparticles as an imaging, targeting and PDT/PTT agent for cancer therapy. *Sci. Rep.* **2016**, *6*, 27421, doi:10.1038/srep27421.
74. Yuan, P.; Luo, Y.; Luo, Y.; Ma, L. A "sandwich" cell culture platform with NIR-responsive dynamic stiffness to modulate macrophage phenotypes. *Biomater. Sci.* **2021**, *9*, 2553–2561, doi:10.1039/d0bm02194f.
75. Liu, C.; Ruan, C.; Shi, R.; Jiang, B.-P.; Ji, S.-C.; Shen, X.-C. A near infrared-modulated thermosensitive hydrogel for stabilization of indocyanine green and combinatorial anticancer phototherapy. *Biomater. Sci.* **2019**, *7*, 1705–1715, doi:10.1039/c8bm01541d.
76. Lu, J.; Cai, L.; Dai, Y.; Liu, Y.; Zuo, F.; Ni, C.; Shi, M.; Li, J. Polydopamine-based Nanoparticles for Photothermal Therapy/Chemotherapy and their Synergistic Therapy with Autophagy Inhibitor to Promote Antitumor Treatment. *Chem. Rec.* **2021**, *21*, 781–796, doi:10.1002/tcr.202000170.
77. Wang, C.; Zhao, N.; Yuan, W. NIR/Thermoresponsive Injectable Self-Healing Hydrogels Containing Polydopamine Nanoparticles for Efficient Synergistic Cancer Thermochemotherapy. *ACS Appl. Mater. Interfaces* **2020**, *12*, 9118–9131, doi:10.1021/acsami.9b23536.

78. Zhou, L.; Ge, J.; Wang, M.; Chen, M.; Cheng, W.; Ji, W.; Lei, B. Injectable muscle-adhesive antioxidant conductive photothermal bioactive nanomatrix for efficiently promoting full-thickness skeletal muscle regeneration. *Bioact. Mater.* **2021**, *6*, 1605–1617, doi:10.1016/j.bioactmat.2020.11.005.
79. Geng, S.; Zhao, H.; Zhan, G.; Zhao, Y.; Yang, X. Injectable in Situ Forming Hydrogels of Thermosensitive Polypyrrole Nanoplatforms for Precisely Synergistic Photothermo-Chemotherapy. *ACS Appl. Mater. Interfaces* **2020**, *12*, 7995–8005, doi:10.1021/acsami.9b22654.
80. Hsiao, C.-W.; Chuang, E.-Y.; Chen, H.-L.; Wan, D.; Korupalli, C.; Liao, Z.-X.; Chiu, Y.-L.; Chia, W.-T.; Lin, K.-J.; Sung, H.-W. Photothermal tumor ablation in mice with repeated therapy sessions using NIR-absorbing micellar hydrogels formed in situ. *Biomaterials* **2015**, *56*, 26–35, doi:10.1016/j.biomaterials.2015.03.060.
81. He, X.Y.; Sun, A.; Li, T.; Qian, Y.J.; Qian, H.; Ling, Y.F.; Zhang, L.H.; Liu, Q.Y.; Peng, T.; Qian, Z. Mussel-inspired antimicrobial gelatin/chitosan tissue adhesive rapidly activated in situ by H2O2/ascorbic acid for infected wound closure. *Carbohydr. Polym.* **2020**, *247*, 116692, doi:10.1016/j.carbpol.2020.116692.
82. Huang, S.; Liu, H.; Liao, K.; Hu, Q.; Guo, R.; Deng, K. Functionalized GO Nanovehicles with Nitric Oxide Release and Photothermal Activity-Based Hydrogels for Bacteria-Infected Wound Healing. *ACS Appl. Mater. Interfaces* **2020**, *12*, 28952–28964, doi:10.1021/acsami.0c04080.
83. Zhou, L.; Xi, Y.; Xue, Y.; Wang, M.; Liu, Y.; Guo, Y.; Lei, B. Injectable Self-Healing Antibacterial Bioactive Polypeptide-Based Hybrid Nanosystems for Efficiently Treating Multidrug Resistant Infection, Skin-Tumor Therapy, and Enhancing Wound Healing. *Adv. Funct. Mater.* **2019**, *29*, 29, doi:10.1002/adfm.201806883.
84. Xu, Q.; Chang, M.; Zhang, Y.; Wang, E.; Xing, M.; Gao, L.; Huan, Z.; Guo, F.; Chang, J. PDA/Cu Bioactive Hydrogel with "Hot Ions Effect" for Inhibition of Drug-Resistant Bacteria and Enhancement of Infectious Skin Wound Healing. *ACS Appl. Mater. Interfaces* **2020**, *12*, 31255–31269, doi:10.1021/acsami.0c08890.
85. Yin, J.; Han, Q.; Zhang, J.; Liu, Y.; Gan, X.; Xie, K.; Xie, L.; Deng, Y. MXene-Based Hydrogels Endow Polyetheretherketone with Effective Osteogenicity and Combined Treatment of Osteosarcoma and Bacterial Infection. *ACS Appl. Mater. Interfaces* **2020**, *12*, 45891–45903, doi:10.1021/acsami.0c14752.
86. Liu, J.; Pu, H.; Liu, S.; Kan, J.; Jin, C. Synthesis, characterization, bioactivity and potential application of phenolic acid grafted chitosan: A review. *Carbohydr. Polym.* **2017**, *174*, 999–1017, doi:10.1016/j.carbpol.2017.07.014.
87. Ryu, J.H.; Hong, S.; Lee, H. Bio-inspired adhesive catechol-conjugated chitosan for biomedical applications: A mini review. *Acta Biomater.* **2015**, *27*, 101–115, doi:10.1016/j.actbio.2015.08.043.
88. Cen, D.; Wan, Z.; Fu, Y.; Pan, H.; Xu, J.; Wang, Y.; Wu, Y.; Li, X.; Cai, X. Implantable fibrous 'patch' enabling preclinical chemo-photothermal tumor therapy. *Colloids Surf. B Biointerfaces* **2020**, *192*, 111005, doi:10.1016/j.colsurfb.2020.111005.
89. Tong, X.; Qi, X.; Mao, R.; Pan, W.; Zhang, M.; Wu, X.; Chen, G.; Shen, J.; Deng, H.; Hu, R. Construction of functional curdlan hydrogels with bio-inspired polydopamine for synergistic periodontal antibacterial therapeutics. *Carbohydr. Polym.* **2020**, *245*, 116585, doi:10.1016/j.carbpol.2020.116585.
90. Liu, Y.; Fan, Q.; Huo, Y.; Liu, C.; Li, B.; Li, Y. Construction of a Mesoporous Polydopamine@GO/Cellulose Nanofibril Composite Hydrogel with an Encapsulation Structure for Controllable Drug Release and Toxicity Shielding. *ACS Appl. Mater. Interfaces* **2020**, *12*, 57410–57420, doi:10.1021/acsami.0c15465.
91. Kim, S.; Seo, J.-H.; Jeong, D.I.; Yang, M.; Lee, S.Y.; Lee, J.; Cho, H.-J. Fenton-like reaction, glutathione reduction, and photothermal ablation-built-in hydrogels crosslinked by cupric sulfate for loco-regional cancer therapy. *Biomater. Sci.* **2021**, *9*, 847–860, doi:10.1039/d0bm01470b.
92. Li, L.; Zeng, Z.; Chen, Z.; Gao, R.; Pan, L.; Deng, J.; Ye, X.; Zhang, J.; Zhang, S.; Mei, C.; et al. Microenvironment-Triggered Degradable Hydrogel for Imaging Diagnosis and Combined Treatment of Intraocular Choroidal Melanoma. *ACS Nano* **2020**, *14*, 15403–15416, doi:10.1021/acsnano.0c06000.
93. Liang, Y.; Zhao, X.; Hu, T.; Chen, B.; Yin, Z.; Ma, P.X.; Guo, B. Adhesive Hemostatic Conducting Injectable Composite Hydrogels with Sustained Drug Release and Photothermal Antibacterial Activity to Promote Full-Thickness Skin Regeneration During Wound Healing. *Small* **2019**, *15*, e1900046, doi:10.1002/smll.201900046.
94. Han, D.; Li, Y.; Liu, X.; Li, B.; Han, Y.; Zheng, Y.; Yeung, K.W.K.; Li, C.; Cui, Z.; Liang, Y.; et al. Rapid bacteria trapping and killing of metal-organic frameworks strengthened photo-responsive hydrogel for rapid tissue repair of bacterial infected wounds. *Chem. Eng. J.* **2020**, *396*, 125194, doi:10.1016/j.cej.2020.125194.
95. Tao, B.; Lina, C.; Yuana, Z.; Hea, Y.; Chena, M.; Lia, K.; Hua, J.; Yanga, Y.; Xiaa, Z.; Caiab, K. Near infrared light-triggered on-demand Cur release from Gel-PDA@Cur composite hydrogel for antibacterial wound healing. *Chem. Eng. J.* **2021**, *403*, 126182, doi:10.1016/j.cej.2020.126182.
96. Li, J.; Liu, X.; Zhou, Z.; Tan, L.; Wang, X.; Zheng, Y.; Han, Y.; Chen, D.-F.; Yeung, K.W.K.; Cui, Z.; et al. Lysozyme-Assisted Photothermal Eradication of Methicillin-Resistant Staphylococcus aureus Infection and Accelerated Tissue Repair with Natural Melanosome Nanostructures. *ACS Nano* **2019**, *13*, 11153–11167, doi:10.1021/acsnano.9b03982.
97. Liu, Y.M.; Ma, W.S.; Wei, Y.X.; Xu, Y.H. Photothermal Effect-based Cytotoxic Ability of Melanin from Mytilus edulis Shells to Heal Wounds Infected with Drug-resistant Bacteria in vivo. *Biomed. Environ. Sci.* **2020**, *33*, 471–483, doi:10.3967/bes2020.052.
98. Xu, Y.; Zhao, S.; Weng, Z.; Zhang, W.; Wan, X.; Cui, T.; Ye, J.; Liao, L.; Wang, X. Jelly-Inspired Injectable Guided Tissue Regeneration Strategy with Shape Auto-Matched and Dual-Light-Defined Antibacterial/Osteogenic Pattern Switch Properties. *ACS Appl. Mater. Interfaces* **2020**, *12*, 54497–54506, doi:10.1021/acsami.0c18070.

99. Chen, Y.; Zhang, Y.; Mensaha, A.; Li, D.; Wang, Q.; Wei, Q. A plant-inspired long-lasting adhesive bilayer nanocomposite hydrogel based on redox-active Ag/Tannic acid-Cellulose nanofibers. *Carbohydr. Polym.* **2021**, *255*, 117508, doi:10.1016/j.carbpol.2020.117508.
100. Qiao, Y.; He, J.; Chen, W.; Yu, Y.; Li, W.; Du, Z.; Xie, T.; Ye, Y.; Hua, S.Y.; Zhong, D.; et al. Light-Activatable Synergistic Therapy of Drug-Resistant Bacteria-Infected Cutaneous Chronic Wounds and Nonhealing Keratitis by Cupriferous Hollow Nanoshells. *ACS Nano* **2020**, *14*, 3299–3315, doi:10.1021/acsnano.9b08930.
101. Yougbaré, S.; Mutalik, C.; Krisnawati, D.I.; Kristanto, H.; Jazidie, A.; Nuh, M.; Cheng, T.-M.; Kuo, T.-R. Nanomaterials for the Photothermal Killing of Bacteria. *Nanomaterials* **2020**, *10*, 1123, doi:10.3390/nano10061123.
102. Chen, S.; Tang, F.; Tang, L.; Li, L. Synthesis of Cu-Nanoparticle Hydrogel with Self-Healing and Photothermal Properties. *ACS Appl. Mater. Interfaces* **2017**, *9*, 20895–20903, doi:10.1021/acsami.7b04956.
103. Kong, Y.; Hou, Z.; Zhou, L.; Zhang, P.; Ouyang, Y.; Wang, P.; Chen, Y.; Luo, X. Injectable Self-Healing Hydrogels Containing CuS Nanoparticles with Abilities of Hemostasis, Antibacterial activity, and Promoting Wound Healing. *ACS Biomater. Sci. Eng.* **2021**, *7*, 335–349, doi:10.1021/acsbiomaterials.0c01473.
104. Zhang, X.; Zhang, G.; Zhang, H.; Liu, X.; Shi, J.; Shi, H.; Yao, X.; Chu, P.K. A bifunctional hydrogel incorporated with CuS@MoS2 microspheres for disinfection and improved wound healing. *Chem. Eng. J.* **2020**, *382*, 122849, doi:10.1016/j.cej.2019.122849.
105. Chambre, L.; Rosselle, L.; Barras, A.; Aydin, D.; Loczechin, A.; Gunbay, S.; Sanyal, R.; Skandrani, N.; Metzler-Nolte, N.; Bandow, J.E.; et al. Photothermally Active Cryogel Devices for Effective Release of Antimicrobial Peptides: On-Demand Treatment of Infections. *ACS Appl. Mater. Interfaces* **2020**, *12*, 56805–56814, doi:10.1021/acsami.0c17633.
106. Liang, Y.; Chen, B.; Li, M.; He, J.; Yin, Z.; Guo, B. Injectable Antimicrobial Conductive Hydrogels for Wound Disinfection and Infectious Wound Healing. *Biomacromolecules* **2020**, *21*, 1841–1852, doi:10.1021/acs.biomac.9b01732.
107. Qiao, B.; Pang, Q.; Yuan, P.; Luo, Y.; Ma, L. Smart wound dressing for infection monitoring and NIR-triggered antibacterial treatment. *Biomater. Sci.* **2020**, *8*, 1649–1657, doi:10.1039/c9bm02060h.
108. Howaili, F.; Özliseli, E.; Küçüktürkmen, B.; Razavi, S.M.; Sadeghizadeh, M.; Rosenholm, J.M. Stimuli-Responsive, Plasmonic Nanogel for Dual Delivery of Curcumin and Photothermal Therapy for Cancer Treatment. *Front. Chem.* **2021**, *8*, 602941, doi:10.3389/fchem.2020.602941.
109. Xi, Y.; Ge, J.; Wang, M.; Chen, M.; Niu, W.; Cheng, W.; Xue, Y.; Lin, C.; Lei, B. Bioactive Anti-inflammatory, Antibacterial, Antioxidative Silicon-Based Nanofibrous Dressing Enables Cutaneous Tumor Photothermo-Chemo Therapy and Infection-Induced Wound Healing. *ACS Nano* **2020**, *14*, 2904–2916, doi:10.1021/acsnano.9b07173.
110. Liang, Y.; Zhao, X.; Hu, T.; Han, Y.; Guo, B. Mussel-inspired, antibacterial, conductive, antioxidant, injectable composite hydrogel wound dressing to promote the regeneration of infected skin. *J. Colloid Interface Sci.* **2019**, *556*, 514–528, doi:10.1016/j.jcis.2019.08.083.
111. Yang, N.; Zhu, M.; Xu, G.; Liu, N.; Yu, C. A near-infrared light-responsive multifunctional nanocomposite hydrogel for efficient and synergistic antibacterial wound therapy and healing promotion. *J. Mater. Chem. B* **2020**, *8*, 3908–3917, doi:10.1039/d0tb00361a.
112. Sheng, L.; Zhang, Z.; Zhang, Y.; Wang, E.; Ma, B.; Xu, Q.; Ma, L.; Zhang, M.; Pei, G.; Chang, J. A novel "hot spring"-mimetic hydrogel with excellent angiogenic properties for chronic wound healing. *Biomaterials* **2021**, *264*, 120414, doi:10.1016/j.biomaterials.2020.120414.
113. Li, M.; Liu, X.; Tan, L.; Cui, Z.; Yang, X.; Li, Z.; Zheng, Y.; Yeung, K.W.K.; Chu, P.K.; Wu, S. Noninvasive rapid bacteria-killing and acceleration of wound healing through photothermal/photodynamic/copper ion synergistic action of a hybrid hydrogel. *Biomater. Sci.* **2018**, *6*, 2110–2121, doi:10.1039/c8bm00499d.
114. Ma, B.; Dang, W.; Yang, Z.; Chang, J.; Wu, C. MoS_2 Nanoclusters-based biomaterials for disease- impaired wound therapy. *Appl. Mater. Today* **2020**, *20*, 100735, doi:10.1016/j.apmt.2020.100735.
115. Zhou, W.; Zi, L.; Cen, Y.; You, C.; Tian, M. Copper Sulfide Nanoparticles-Incorporated Hyaluronic Acid Injectable Hydrogel with Enhanced Angiogenesis to Promote Wound Healing. *Front. Bioeng. Biotechnol.* **2020**, *8*, 417, doi:10.3389/fbioe.2020.00417.
116. Zhang, X.; Chen, G.; Liu, Y.; Sun, L.; Zhao, Y. Black Phosphorus-Loaded Separable Microneedles as Responsive Oxygen Delivery Carriers for Wound Healing. *ACS Nano* **2020**, *14*, 5901–5908, doi:10.1021/acsnano.0c01059.
117. Li, W.-P.; Su, C.-H.; Wang, S.-J.; Tsai, F.-J.; Chang, C.-T.; Liao, M.-C.; Yu, C.-C.; Tran, T.-T.V.; Lee, C.-N.; Chiu, W.-T.; et al. CO_2 Delivery to Accelerate Incisional Wound Healing Following Single Irradiation of Near-Infrared Lamp on the Coordinated Colloids. *ACS Nano* **2017**, *11*, 5826–5835, doi:10.1021/acsnano.7b01442.
118. Xie, G.; Zhou, N.; Gao, Y.; Du, S.; Du, H.; Tao, J.; Zhang, L.; Zhu, J. On-demand release of CO_2 from photothermal hydrogels for accelerating skin wound healing. *Chem. Eng. J.* **2021**, *403*, 126353, doi:10.1016/j.cej.2020.126353.
119. Veith, A.; Henderson, K.; Spencer, A.; Sligar, A.D.; Baker, A.B. Therapeutic strategies for enhancing angiogenesis in wound healing. *Adv. Drug Deliv. Rev.* **2019**, *146*, 97–125, doi:10.1016/j.addr.2018.09.010.
120. Phan, L.; Vo, T.; Hoang, T.; Cho, S. Graphene Integrated Hydrogels Based Biomaterials in Photothermal Biomedicine. *Nanomaterials* **2021**, *11*, 906, doi:10.3390/nano11040906.
121. Liu, H.; Zhu, X.; Guo, H.; Huang, H.; Huang, S.; Huang, S.; Xue, W.; Zhu, P.; Guo, R. Nitric oxide released injectable hydrogel combined with synergistic photothermal therapy for antibacterial and accelerated wound healing. *Appl. Mater. Today* **2020**, *20*, 100781, doi:10.1016/j.apmt.2020.100781.
122. Chen, J.; Shi, Z.-D.; Ji, X.; Morales, J.; Zhang, J.; Kaur, N.; Wang, S. Enhanced Osteogenesis of Human Mesenchymal Stem Cells by Periodic Heat Shock in Self-Assembling Peptide Hydrogel. *Tissue Eng. Part A* **2013**, *19*, 716–728, doi:10.1089/ten.tea.2012.0070.

123. Yang, B.; Yin, J.; Chen, Y.; Pan, S.; Yao, H.; Gao, Y.; Shi, J. 2D-Black-Phosphorus-Reinforced 3D-Printed Scaffolds:A Stepwise Countermeasure for Osteosarcoma. *Adv. Mater.* **2018**, *30*, doi:10.1002/adma.201705611.
124. Shao, J.; Ruan, C.; Xie, H.; Chu, P.K.; Yu, X. Photochemical Activity of Black Phosphorus for Near-Infrared Light Controlled In Situ Biomineralization. *Adv. Sci.* **2020**, *7*, 2000439, doi:10.1002/advs.202000439.
125. Miao, Y.; Shi, X.; Li, Q.; Hao, L.; Liu, L.; Liu, X.; Chen, Y.; Wang, Y. Engineering natural matrices with black phosphorus nanosheets to generate multi-functional therapeutic nanocomposite hydrogels. *Biomater. Sci.* **2019**, *7*, 4046–4059, doi:10.1039/c9bm01072f.
126. Zhao, P.-P.; Ge, Y.-W.; Liu, X.-L.; Ke, Q.-F.; Zhang, J.-W.; Zhu, Z.-A.; Guo, Y.-P. Ordered arrangement of hydrated GdPO4 nanorods in magnetic chitosan matrix promotes tumor photothermal therapy and bone regeneration against breast cancer bone metastases. *Chem. Eng. J.* **2020**, *381*, 122694, doi:10.1016/j.cej.2019.122694.
127. Sanchez-Casanova, S.; Martin-Saavedra, F.M.; Escudero-Duch, C.; Uceda, M.I.F.; Prieto, M.; Arruebo, M.; Acebo, P.; Fabiilli, M.L.; Franceschi, R.T.; Vilaboa, N. Local delivery of bone morphogenetic protein-2 from near infrared-responsive hydrogels for bone tissue regeneration. *Biomaterials* **2020**, *241*, 119909, doi:10.1016/j.biomaterials.2020.119909.
128. Pensak, M.; Hong, S.; Dukas, A.; Tinsley, B.; Drissi, H.; Tang, A.; Côté, M.; Sugiyama, O.; Lichtler, A.; Rowe, D.; et al. The role of transduced bone marrow cells overexpressing BMP-2 in healing critical-sized defects in a mouse femur. *Gene Ther.* **2015**, *22*, 467–475, doi:10.1038/gt.2015.14.
129. Ma, L.; Feng, X.; Liang, H.; Wang, K.; Song, Y.; Tan, L.; Wang, B.; Luo, R.; Liao, Z.; Li, G.; et al. A novel photothermally controlled multifunctional scaffold for clinical treatment of osteosarcoma and tissue regeneration. *Mater. Today* **2020**, *36*, 48–62, doi:10.1016/j.mattod.2019.12.005.
130. Pan, W.; Dai, C.; Li, Y.; Yin, Y.; Gong, L.; Machuki, J.O.; Yang, Y.; Qiu, S.; Guo, K.; Gao, F. PRP-chitosan thermoresponsive hydrogel combined with black phosphorus nanosheets as injectable biomaterial for biotherapy and phototherapy treatment of rheumatoid arthritis. *Biomaterials* **2020**, *239*, 119851, doi:10.1016/j.biomaterials.2020.119851.
131. Gao, G.; Jiang, Y.-W.; Jia, H.-R.; Wu, F.-G. Near-infrared light-controllable on-demand antibiotics release using thermo-sensitive hydrogel-based drug reservoir for combating bacterial infection. *Biomaterials* **2019**, *188*, 83–95, doi:10.1016/j.biomaterials.2018.09.045.
132. Xu, X.; Liu, X.; Tan, L.; Cui, Z.; Yang, X.; Zhu, S.; Li, Z.; Yuan, X.; Zheng, Y.; Yeung, K.W.K.; et al. Controlled-temperature photothermal and oxidative bacteria killing and acceleration of wound healing by polydopamine-assisted Au-hydroxyapatite nanorods. *Acta Biomater.* **2018**, *77*, 352–364, doi:10.1016/j.actbio.2018.07.030.
133. Zhao, X.; Liang, Y.; Huang, Y.; He, J.; Han, Y.; Guo, B. Physical Double-Network Hydrogel Adhesives with Rapid Shape Adaptability, Fast Self-Healing, Antioxidant and NIR/pH Stimulus-Responsiveness for Multidrug-Resistant Bacterial Infection and Removable Wound Dressing. *Adv. Funct. Mater.* **2020**, *30*, 133, doi:10.1002/adfm.201910748.
134. Wang, S.; Zheng, H.; Zhou, L.; Cheng, F.; Liu, Z.; Zhang, H.; Zhang, Q. Injectable redox and light responsive MnO2 hybrid hydrogel for simultaneous melanoma therapy and multidrug-resistant bacteria-infected wound healing. *Biomaterials* **2020**, *260*, 120314, doi:10.1016/j.biomaterials.2020.120314.
135. Yu, Y.; Li, P.; Zhu, C.; Ning, N.; Zhang, S.; Vancso, G.J. Multifunctional and Recyclable Photothermally Responsive Cryogels as Efficient Platforms for Wound Healing. *Adv. Funct. Mater.* **2019**, *29*, 29, doi:10.1002/adfm.201904402.
136. Zhang, H.; Sun, X.; Wang, J.; Zhang, Y.; Dong, M.; Bu, T.; Li, L.; Liu, Y.; Wang, L. Multifunctional Injectable Hydrogel Dressings for Effectively Accelerating Wound Healing: Enhancing Biomineralization Strategy. *Adv. Funct. Mater.* **2021**, 2100093, doi:10.1002/adfm.202100093.
137. Xi, J.; Wu, Q.; Xu, Z.; Wang, Y.; Zhu, B.; Fan, L.; Gao, L. Aloe-Emodin/Carbon Nanoparticle Hybrid Gels with Light-Induced and Long-Term Antibacterial Activity. *ACS Biomater. Sci. Eng.* **2018**, *4*, 4391–4400, doi:10.1021/acsbiomaterials.8b00972.
138. Ma, H.; Zhou, Q.; Chang, J.; Wu, C. Grape Seed-Inspired Smart Hydrogel Scaffolds for Melanoma Therapy and Wound Healing. *ACS Nano* **2019**, *13*, 4302–4311, doi:10.1021/acsnano.8b09496.
139. Wang, M.; Zhu, H.; Shen, J. Synthesis and molecular dynamics simulation of CuS@GO–CS hydrogel for enhanced photothermal antibacterial effect. *New J. Chem.* **2021**, *45*, 6895–6903, doi:10.1039/d0nj05891b.
140. Zhou, L.; Chen, F.; Hou, Z.; Chen, Y.; Luo, X. Injectable self-healing CuS nanoparticle complex hydrogels with antibacterial, anti-cancer, and wound healing properties. *Chem. Eng. J.* **2021**, *409*, 128224, doi:10.1016/j.cej.2020.128224.
141. Martín-Saavedra, F.; Escudero-Duch, C.; Prieto, M.; Sánchez-Casanova, S.; López, D.; Arruebo, M.; Voellmy, R.; Santamaría, J.; Vilaboa, N. Pro-angiogenic near infrared-responsive hydrogels for deliberate transgene expression. *Acta Biomater.* **2018**, *78*, 123–136, doi:10.1016/j.actbio.2018.08.006.
142. Sun, J.; Tan, H.; Liu, H.; Jin, D.; Yin, M.; Lin, H.; Qu, X.; Liu, C. A reduced polydopamine nanoparticle-coupled sprayable PEG hydrogel adhesive with anti-infection activity for rapid wound sealing. *Biomater. Sci.* **2020**, *8*, 6946–6956, doi:10.1039/d0bm01213k.
143. Chu, X.; Zhang, P.; Wang, Y.; Sun, B.; Liu, Y.; Zhang, Q.; Feng, W.; Li, Z.; Li, K.; Zhou, N.; et al. Near-infrared carbon dot-based platform for bioimaging and photothermal/photodynamic/quaternary ammonium triple synergistic sterilization triggered by single NIR light source. *Carbon* **2021**, *176*, 126–138, doi:10.1016/j.carbon.2021.01.119.
144. Deng, H.; Sun, J.; Yu, Z.; Guo, Z.; Xu, C. Low-intensity near-infrared light-triggered spatiotemporal antibiotics release and hyperthermia by natural polysaccharide-based hybrid hydrogel for synergistic wound disinfection. *Mater. Sci. Eng. C* **2021**, *118*, 111530, doi:10.1016/j.msec.2020.111530.

145. Wang, H.; Zhou, S.; Guo, L.; Wang, Y.; Feng, L. Intelligent Hybrid Hydrogels for Rapid In Situ Detection and Photothermal Therapy of Bacterial Infection. *ACS Appl. Mater. Interfaces* **2020**, *12*, 39685–39694, doi:10.1021/acsami.0c12355.
146. Xu, C.; Akakuru, O.U.; Ma, X.; Zheng, J.; Zheng, J.; Wu, A. Nanoparticle-Based Wound Dressing: Recent Progress in the Detection and Therapy of Bacterial Infections. *Bioconjugate Chem.* **2020**, *31*, 1708–1723, doi:10.1021/acs.bioconjchem.0c00297.
147. Wang, X.; Fang, J.; Zhu, W.; Zhong, C.; Ye, D.; Zhu, M.; Lu, X.; Zhao, Y.; Ren, F. Bioinspired Highly Anisotropic, Ultrastrong and Stiff, and Osteoconductive Mineralized Wood Hydrogel Composites for Bone Repair. *Adv. Funct. Mater.* **2021**, 2010068, doi:10.1002/adfm.202010068.
148. Li, Y.; Liu, X.; Li, B.; Zheng, Y.; Han, Y.; Chen, D.-F.; Yeung, K.W.K.; Cui, Z.; Liang, Y.; Li, Z.; et al. Near-Infrared Light Triggered Phototherapy and Immunotherapy for Elimination of Methicillin-Resistant Staphylococcus aureus Biofilm Infection on Bone Implant. *ACS Nano* **2020**, *14*, 8157–8170, doi:10.1021/acsnano.0c01486.
149. Wan, Z.; Zhang, P.; Lv, L.; Zhou, Y. NIR light-assisted phototherapies for bone-related diseases and bone tissue regeneration: A systematic review. *Theranostics* **2020**, *10*, 11837–11861, doi:10.7150/thno.49784.
150. Luo, S.; Wu, J.; Jia, Z.; Tang, P.; Sheng, J.; Xie, C.; Liu, C.; Gan, D.; Hu, D.; Zheng, W.; et al. An Injectable, Bifunctional Hydrogel with Photothermal Effects for Tumor Therapy and Bone Regeneration. *Macromol. Biosci.* **2019**, *19*, e1900047, doi:10.1002/mabi.201900047.
151. Xue, Y.; Niu, W.; Wang, M.; Chen, M.; Guo, Y.; Lei, B. Engineering a Biodegradable Multifunctional Antibacterial Bioactive Nanosystem for Enhancing Tumor Photothermo-Chemotherapy and Bone Regeneration. *ACS Nano* **2019**, *14*, 442–453, doi:10.1021/acsnano.9b06145.
152. Zhang, X.; Ma, J. Photothermal effect of 3D printed hydroxyapatite composite scaffolds incorporated with graphene nanoplatelets. *Ceram. Int.* **2021**, *47*, 6336–6340, doi:10.1016/j.ceramint.2020.10.212.
153. Wang, X.; Guo, W.; Li, L.; Yu, F.; Li, J.; Liu, L.; Fang, B.; Xia, L. Photothermally triggered biomimetic drug delivery of Teriparatide via reduced graphene oxide loaded chitosan hydrogel for osteoporotic bone regeneration. *Chem. Eng. J.* **2021**, *413*, 127413, doi:10.1016/j.cej.2020.127413.
154. Yang, C.; Gao, X.; Younis, M.R.; Blum, N.T.; Lei, S.; Zhang, D.; Luo, Y.; Huang, P.; Lin, J. Non-invasive monitoring of in vivo bone regeneration based on alkaline phosphatase-responsive scaffolds. *Chem. Eng. J.* **2021**, *408*, 127959, doi:10.1016/j.cej.2020.127959.